Supplementary Figure Legends:

Figure S1: ACME-dissociated cell cytometry profiles in irradiated animals and comparison to trypsin.

A: Flow cytometry ungated and gated profiles of ACME-dissociated cells from non irradiated (left panels) and irradiated (right panels) *S. mediterranea* planarians, stained with DRAQ5 (nucleus) and Concanavalin-A (cytoplasm). The experiment was performed in 3 replicates. Axes are shown in subset logarithmic scale. **B:** Quantification of %G2 cells compared to all gated singlets. The values in the plot correspond to the average of the 3 replicates, and the error bars correspond to the standard deviation. **C:** Flow cytometry ungated and gated profiles of ACME-dissociated cells (top panels) and trypsin-dissociated cells (bottom panels) from *S.mediterranea* planarians stained with DRAQ5 (nucleus). The cytoplasm of ACME-dissociated and trypsin-dissociated cells was stained with Concanavalin-A and Calcein, respectively.

Figure S2: Inference of RIN values.

A: Correlative analysis of RIN values and the % area of the two ribosomal bands compared to the total. The linear correlation is indicated in the chart. **B:** Tables containing the individual values extracted from the RNA samples displayed in Figures 3-4. The individual values not calculated by the RIN algorithm are show in blue as inferred from the linear correlation.

Figure S3: *Nematostella vectensis* metacell analysis.

A: Flow cytometry profiles of ACME-dissociated cells from *Nematostella vectensis,* showing all events (left) and G1/G0 singlets (right). **B:** Expression of 514 variable genes (rows) across 3,899 juvenile *N. vectensis* single cells sorted by metacell and cell type association. Top 30 genes (FC>2) per metacell are included, showing gene functional annotation when available. Transcription factors are highlighted in red. **C:** Total number of RNA molecules (left) and cells (right) per metacell.

Figure S4: SPLiT-seq workflow and sub-library description

A: SPLiT-seq workflow: cells are randomly split in 96-well plates containing unique barcodes. The first RT round captures mRNAs using an anchored-poly dT barcode (BC 1). The second (BC 2) and third barcodes (BC 3, which includes the UMI) are ligated to the cDNA in two subsequent reactions. The last barcode (BC 4) is added in a final PCR reaction after tagmentation. **B:** Structure of the SPLiT-seq library. Paired-end reads (Read 1 and Read 2) and index were sequenced as indicated. **C:** Bioanalyzer profile of the 3 individual sub-libraries described here. **D:** Violin plots showing the distribution of UMI counts per cell in each sub-library for *S. mediterranea* (left) and *D. japonica* (right). **E:** UMAP visualization of *S. mediterranea* cells (top) and *D. japonica* cells (bottom), coloured by sub-library.

Figure S5: Expression of previously published cell type markers in our dataset.

Feature plots of cell type markers from Plass *et al.* in our UMAP visualization of *S. mediterranea* cells.

Figure S6: Expression of germ line progenitor markers.

A: Feature plots of germ line progenitor markers *Smed-eIF3c* and *Smed-nanos* in our *S. mediterranea* dataset and previously published studies: Plass *et al*. (downloaded from https://shiny.mdc-berlin.de/psca/), Fincher *et al*. (downloaded from https://digiworm.wi.mit.edu/) and Zeng *et al*. (downloaded from https://planosphere.stowers.org). **B:** Feature plots of germ line progenitor markers in the *D. japonica* dataset.

Figure S7: Analysis of high UMI-containing cell clusters

A) UMAP visualization of 19,975 ACME-dissociated *S. mediterranea* cells (before >5000 UMI cut-off), and 14,263 ACME-dissociated *D. japonica* cells coloured by UMI content. B) Feature plots of germ line precursor progenitor marker *nanos* in the UMAP visualization of 19,975 *S. mediterranea* cells and 14,263 ACME-dissociated *D. japonica* cells. C) UMAP visualization of the 19,025 ACME-dissociated *S. mediterranea* cells (after >5000 UMI cut-off), and 13,406 ACME-dissociated *D. japonica* cells shown in Fig 7, coloured by UMI content.

Figure S8: Results of downsampling experiments, showing UMI, gene and cluster recovery at a variety of equivalent cutoff points.

Downsampling statistics shown are: Statistics after downsampling García-Castro raw reads to 1,200,007,715 (Plass *et al*. total). Statistics after downsampling all Plass *et al*. reads to 560,518,316 (García-Castro, usable total). Statistics after downsampling both Plass *et al.* and García-Castro results to 10k mapped reads per cell. Also shown are the resulting UMAP representations from these downsampled sets, in the same order as the raw statistics. Note that we observe 40 rather than 41 clusters in our sample when downsampled to approx 88% of original raw read count to match the raw Plass *et al.* number. We see 24 rather than 38 clusters in the Plass *et al*. sample when we downsample these reads to match the number of reads from García-Castro used in analysis (46.7% of the original Plass count). When 10k mapped reads are used per cell, there is no loss of cluster representation in the García-Castro dataset compared to the overall analysis, but 33 (c.f. 38) clusters are seen in the Plass *et al*. data.

Figure S9: **Comparison of results of differential expression analysis, Plass *et al*. vs García-Castro *et al*.**

Comparisons made between neoblast clusters and mature cell types for each dataset as noted. Excellent overlap was seen in recovered genes (74.3 - 84.4% of the DE genes found in ACME-dissociated García-Castro DE analysis were also found in the Trypsin-dissociated Plass *et al*. comparisons). These also show a clear correlation in log fold change values when García-Castro and Plass *et al*. results are compared, in all cell types examined.

Figure S10: Comparison of distribution of UMI counts and genes detected per cluster in this study and Plass *et al*.

A: Violin plots showing the distribution of UMI counts per cluster in ACME-dissociated (left) and trypsin-dissociated (right) *S. mediterranea* cells reanalysed from Plass *et al*. **B:** Violin plots showing the distribution of genes detected per cluster in ACME-dissociated (left) and trypsin-dissociated (right) *S. mediterranea* cells reanalysed from Plass *et al*. Colours of plots match those of the clusters shown in Figs 7A and 8B (ACME and Plass cells respectively) and are ordered according to cluster identity.

Figure S11: Integrative analysis of trypsin- and ACME-dissociated datasets

A: Analysis workflow. **B:** UMAP visualization of 21,610 trypsin-dissociated *S. mediterranea* cells reanalysed from Plass *et al*., coloured by cluster identity and annotated on the basis of marker genes. **C:** UMAP visualisation of 21,610 trypsin-dissociated *S. mediterranea* cells. Cells annotated as germ cells are coloured by transfer labels analysis from ACME-dissociated cells. **D:** Feature plots of germ line progenitor markers *Smed-eIF3c* and *Smed-nanos* in the UMAP visualization of 21,610 trypsin-dissociated *S. mediterranea* cells reanalysed from Plass *et al*. **E:** UMAP visualization of 40,635 cells integrating trypsin-dissociated and ACME-dissociated clusters coloured by transfer labels analysis from trypsin-dissociated cells.

A

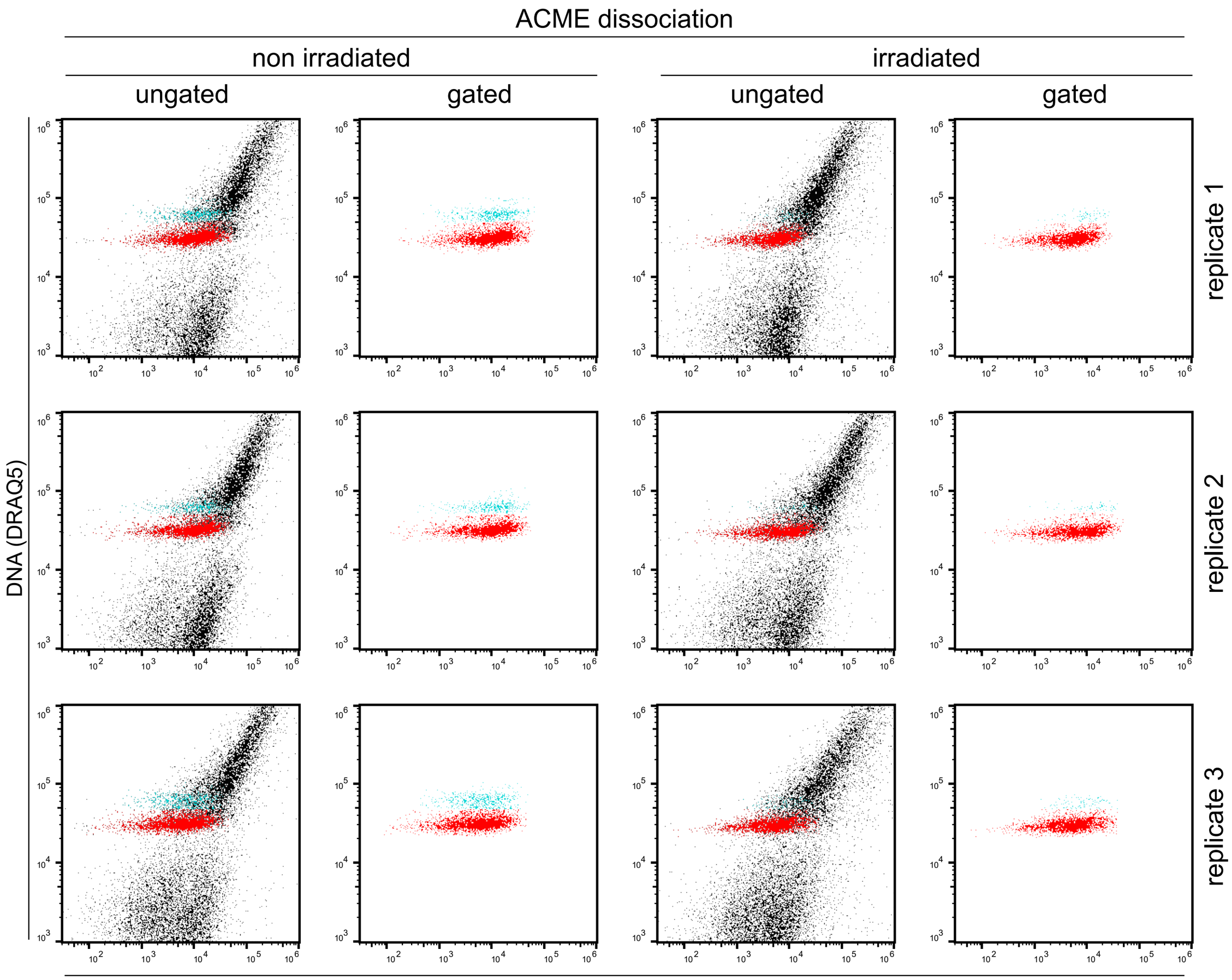
ACME dissociation
non irradiated
irradiated
ungated
gated
ungated
gated
replicate 1
replicate 2
replicate 3
DNA (DRAQ5)
Cytoplasm (Con-A)

B

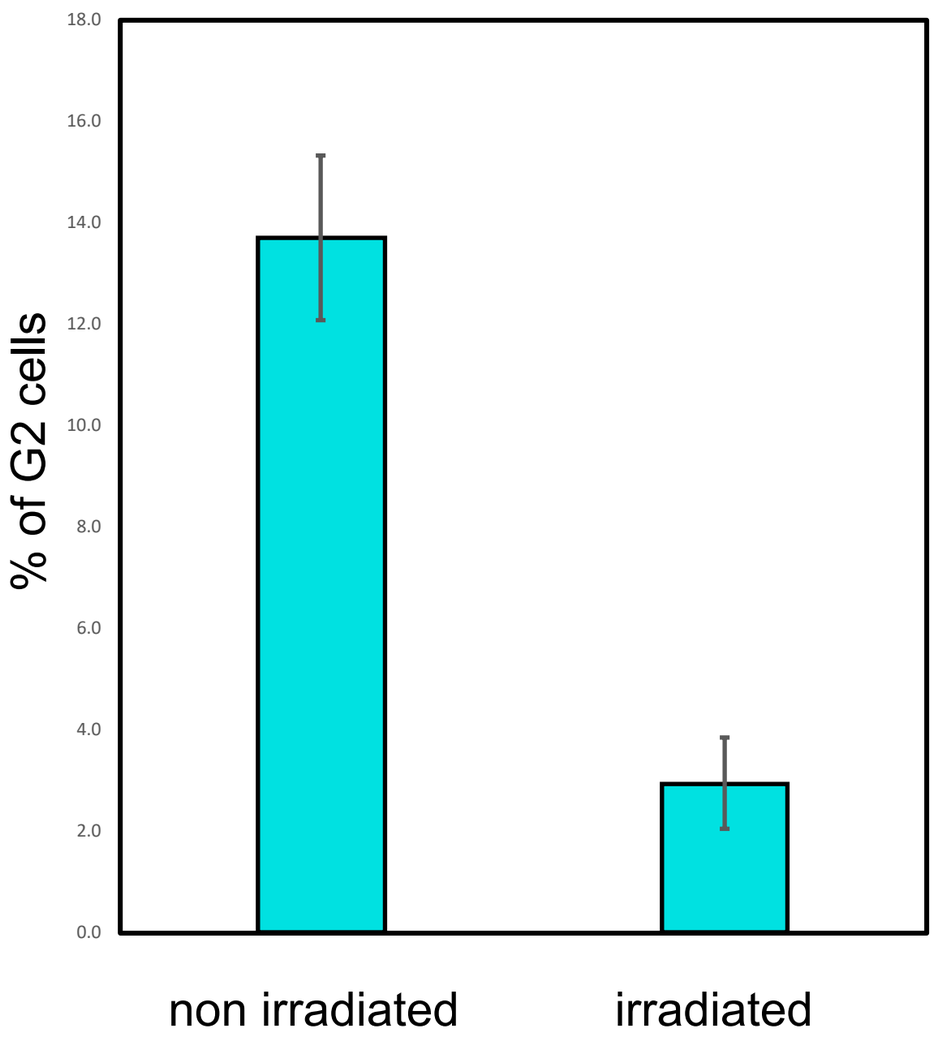
% of G2 cells
18.0
16.0
14.0
12.0
10.0
8.0
6.0
4.0
2.0
0.0
non irradiated
irradiated

C

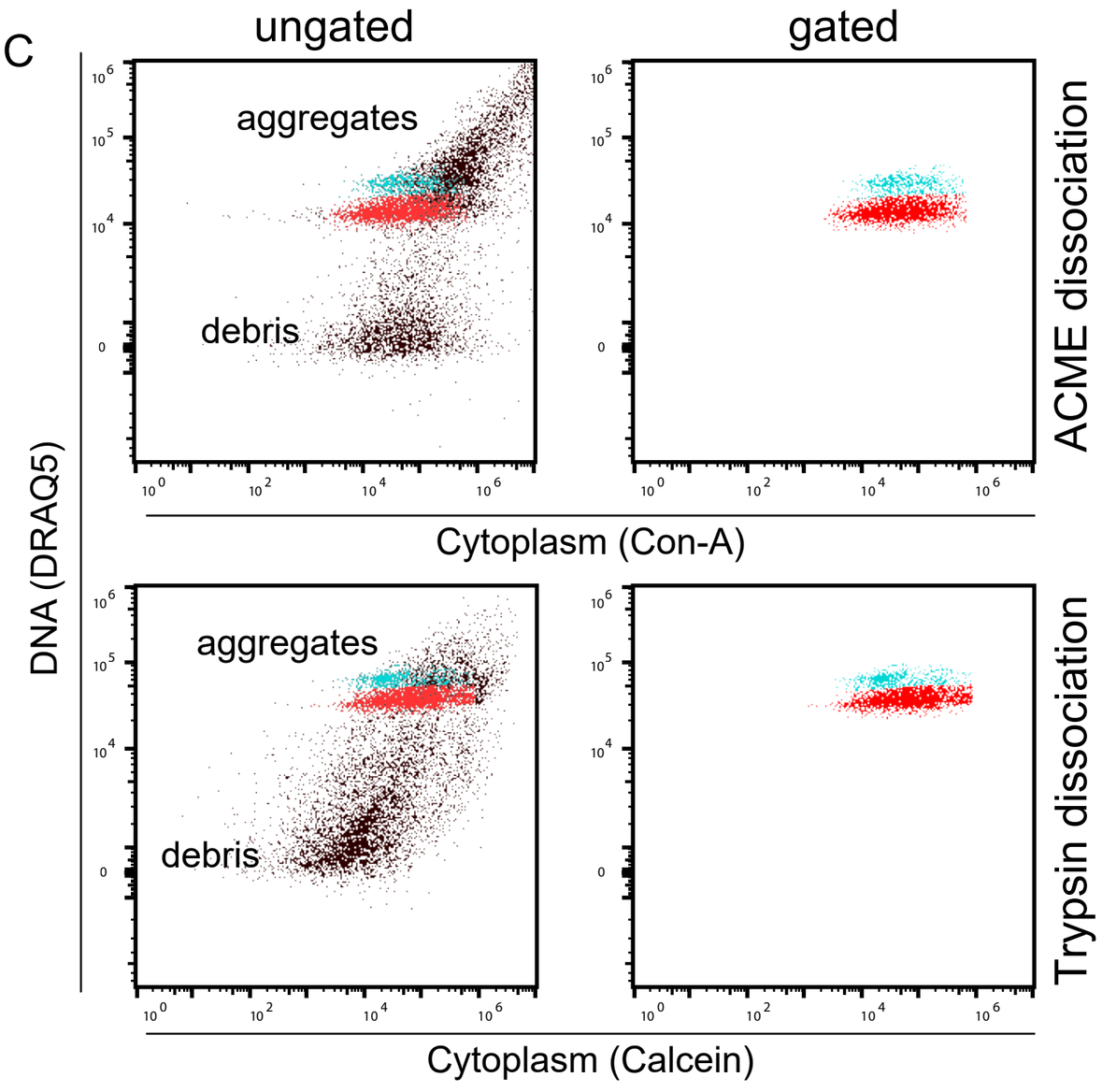
ungated
gated
aggregates
debris
ACME dissociation
DNA (DRAQ5)
Cytoplasm (Con-A)
Trypsin dissociation
Cytoplasm (Calcein)

A

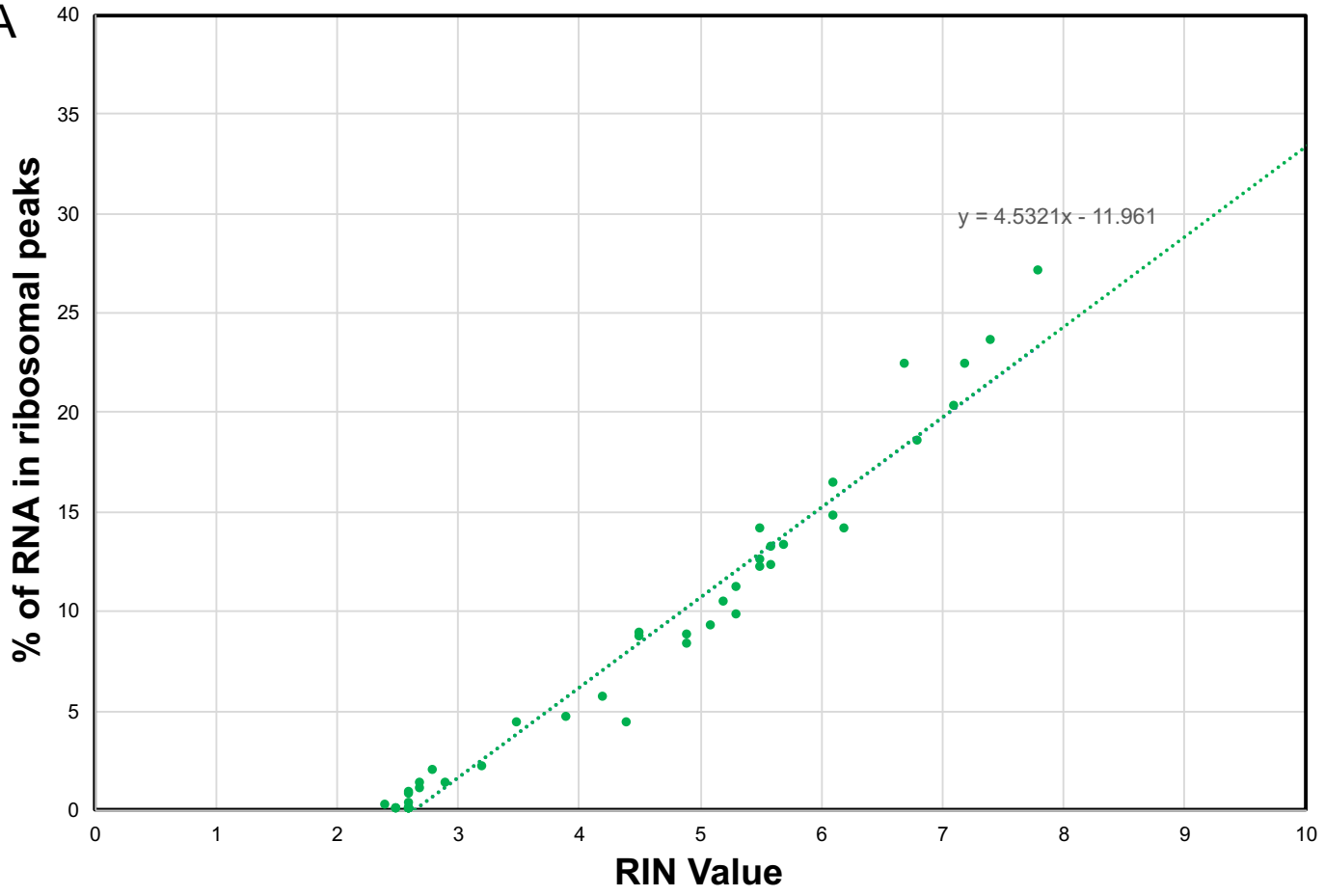

B

Figure 3H	RIN	RNA conc (ng/uL)	% in peaks
t= 0	7.8	143	27
1 hour	3.5	148	4.3
2 hours	3.2	114	2.1
3 hours	2.8	170	1.9
4 hours	2.9	187	1.3
5 hours	2.7	222	1.3
6 hours	2.6	218	0.8

Figure 3I	RIN	RNA conc (ng/uL)	% in peaks
t= 0	7.2	147	22.3
1 hour	6.1	192	14.7
2 hours	4.5	192	8.8
3 hours	4.9	141	8.7
4 hours	5.1	206	9.2
5 hours	4.9	233	8.3
6 hours	4.5	275	8.6

Figure 3K	RIN	RNA conc (ng/uL)	% in peaks
1 cycle	6.7	151	22.3
2 cycles	6.1	205	16.4
3 cycles	5.7	192	13.2
4 cycles	5.5	150	12.5
5 cycles	5.3	162	9.7

Figure 3G	RIN	RNA conc (ng/uL)	% in peaks	Inferred RIN
Control	N/C	105	46.4	10

Figure 3J	RIN	RNA conc (ng/uL)	% in peaks	Inferred RIN
B	N/C	161	28.7	9.0
C	7.4	243	23.5	-
D	4.2	211	5.6	-
E	5.5	292	14.1	-

Figure 4C	RIN	RNA conc (ng/uL)	% in peaks	Inferred RIN
Trypsin	6.2	216	14.1	-
Try + Mace	3.9	272	4.6	-
Try + 0.5 FA	N/C	192	5.5	3.9
Try + 1 FA	2.5	145	0	-
Try + 2 FA	2.5	212	0	-
Try + 3 FA	2.6	210	0	-
Try + 4 FA	2.6	143	0	-

A

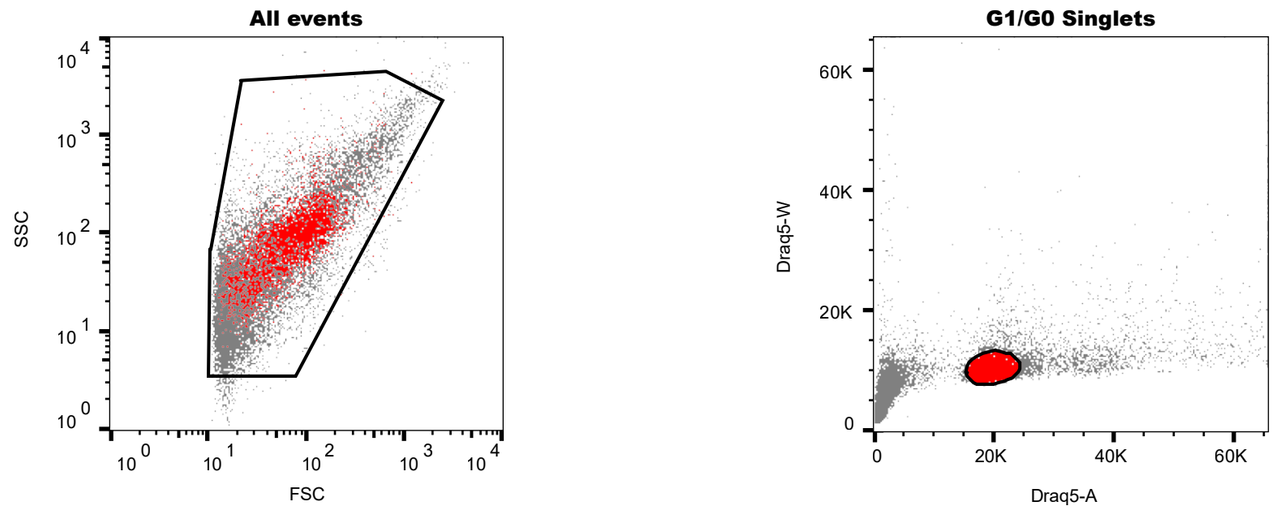
All events
SSC
FSC
G1/G0 Singlets
Draq5-W
Draq5-A
60K
40K
20K
0

B


Nvec_v1g123745 Homeobox/
Nvec_v1g168908 PAX/Homeobox/
Nvec_v1g97005 HLH.HG1.14:PTF1A
Nvec_v1g121965 zf−C2H2.HG3.1:INSM1/INSM2
Nvec_v1g232632 HLH/
Nvec_v1g197394 bZIP.HG1.15:DBP/HLF/TEF
Nvec_v1g233307 Tetraspannin/
Nvec_v1g16815 Ets.HG1.12:ETV1/ETV4/ETV5
Nvec_v1g196609 GATA.HG1.8:GATA1/GATA2/GATA3
Nvec_v1g119550 SET/zf−H2C2_2/zf−H2C2_2/
Nvec_v1g202545 CSD.HG1.5:LIN28A/LIN28B
Nvec_v1g130873 Homeobox.HG4.1:SINE_SIX3/SINE_SIX5
Nvec_v1g205768 Homeobox.HG1.72:PRD_OTP
Nvec_v1g237884 F5_F8_type_C/
Nvec_v1g243338 RHD_Rel.HG2.0:NFAT5/NFATC1/NFATC2/NFA...
Nvec_v1g65438 Forkhead.HG1.8:FOXJ1
Nvec_v1g213483 Tetraspannin/
Nvec_v1g91593 Homeobox.HG2.64:ANTP_GSX1/ANTP_GSX2
Nvec_v1g207820 HMG_box/
Nvec_v1g136184 HLH/
Nvec_v1g160868 Homeobox.HG1.25:POU_POU4F1/POU_POU4F2...
Nvec_v1g91324 Synaptotagmin.HG2.7:MCTP1/MCTP2
Nvec_v1g129231 Runt_Runx.HG1.1:RUNX1/RUNX2/RUNX3
Nvec_v1g233229 bZIP_1/
Nvec_v1g131609 HMGbox_Sox.HG1.9:SOX11/SOX12/SOX4
Nvec_v1g239535 PAX/Homeobox/
Nvec_v1g248021 bZIP.HG3.0:CREBZF
Nvec_v1g243542 Homeobox.HG11.0:CERS_CERS2/CERS_CERS3...
Nvec_v1g86916 HSF.HG1.6:HSF1/HSF2/HSF4
Nvec_v1g19862 DM/
Nvec_v1g238589 bZIP.HG4.1:JUN/JUNB/JUND
Nvec_v1g234494 Actin/
Nvec_v1g246249 HLH.HG2.11:HELT
Nvec_v1g18367 bZIP_Maf/
Nvec_v1g29806 Ets.HG1.16:ETV6/ETV7
Nvec_v1g248713 bZIP_2/
Nvec_v1g86952 bZIP_Maf/
Nvec_v1g92283 IRF.HG1.4:IRF1/IRF2
Nvec_v1g28519 bZIP.HG3.5:CREB3L1/CREB3L2
Nvec_v1g232694 bZIP.HG1.11:FOS/FOSB/FOSL1/FOSL2
Nvec_v1g102092 zf−H2C2_2/zf−H2C2_2/zf−H2C2_2/zf−C2H2...
Nvec_v1g241656 HLH/Hairy_orange/
Nvec_v1g92405 Ets/
Nvec_v1g96685 Fork_head/
Nvec_NVE7724 Gal_Lectin/
Nvec_NVE19743 HLH/
Nvec_NVE7697 Homeobox/
Nvec_v1g108724 Ets.HG1.10:ERG/FEV/FLI1
Nvec_v1g185184 HMG_box/HMG_box/
Nvec_v1g85569 RFX.HG1.1:RFX4/RFX6/RFX8
Nvec_v1g13439 Fcf1/
Nvec_v1g165261 Forkhead.HG1.24:FOXA1/FOXA2/FOXA3
Nvec_v1g80394 Homeobox.HG2.7:ANTP_MSX1/ANTP_MSX2
Nvec_v1g104726 bZIP.HG1.7:CEBPA/CEBPB/CEBPD/CEBPE/CEBPG
Nvec_v1g110792 Homeobox/
Nvec_v1g80187 Homeobox.HG1.68:PRD_PITX1/PRD_PITX2
Nvec_v1g126293 TSP_1/TSP_1/
Nvec_v1g48313 Homeobox.HG2.18:ANTP_NANOG/ANTP_NKX2−...
Nvec_v1g188243 Actin/
Nvec_v1g80365 Homeobox.HG2.60:ANTP_HLX
Nvec_v1g240954 HLH.HG1.39:ID1/ID2/ID3/ID4
Nvec_v1g39924 Homeobox/
Nvec_v1g107027 Ldl_recept_a/Ldl_recept_a/Ldl_recept_...
Nvec_NVE10051 Ldl_recept_a/Ldl_recept_a/Ldl_recept_a/
Nvec_v1g213735 Homeobox.HG1.79:PRD_CRX/PRD_OTX1/PRD_...
Nvec_v1g80243 bZIP_2/
Nvec_v1g113172 Homeobox/
Nvec_v1g205652 Collagen/Collagen/Collagen/Collagen/C...
Nvec_v1g204742 Collagen/Collagen/Collagen/Collagen/C...
Nvec_v1g214570 T−box.HG1.4:TBX1/TBX10
Nvec_NVE9848 HLH/
Nvec_v1g200103 CH/
Nvec_v1g128289 Homeobox.HG2.54:ANTP_MEOX1/ANTP_MEOX2
Nvec_v1g237552 Ferritin/
Nvec_v1g175341 Ferritin/
Nvec_v1g241043 Ig_2/Ig_2/
Nvec_v1g101730 Homeobox.HG2.84:ANTP_HOXA4/ANTP_HOXB4...
Nvec_NVE17354 E2F_TDP.HG1.1:E2F4/E2F5
Nvec_v1g114134 Kunitz_BPTI/
Nvec_v1g175347 Ferritin/
Nvec_v1g210012 Tropomyosin/
Nvec_v1g184228 EF−hand_6/EF−hand_6/
Nvec_v1g160634 EF−hand_6/
Nvec_v1g169611 Actin/
Nvec_v1g204664 HLH/
Nvec_NVE9976 Collagen/
Nvec_v1g95962 bZIP.HG4.1:JUN/JUNB/JUND
Nvec_v1g81344 zf−C2H2_6/zf−H2C2_2/zf−H2C2_2/zf−H2C2...
Nvec_v1g67043 Forkhead.HG1.22:FOXL2
Homeodomains:ANTP_BARX1/ANTP_BARX2
Homeodomains:like:PRD_PAX4/PRD_PAX6:l...
HLH:PTF1A
zf−C2H2:INSM1/INSM2
HLH:like:ID1/ID2/ID3/ID4:likeclu:40
bZIP:DBP/HLF/TEF
Tetraspanin
Ets:ETV1/ETV4/ETV5
GATA:GATA1/GATA2/GATA3
SET:like:PRDM14:likeclu:2
CSD:LIN28A/LIN28B
Homeodomains:SINE_SIX3/SINE_SIX5
Homeodomains:PRD_OTP
EGF−like repeat and discoidin I−like ...
RHD_Rel:NFAT5/NFATC1/NFATC2/NFATC3/NF...
Forkhead:FOXJ1
Tetraspanin−7
Homeodomains:ANTP_GSX1/ANTP_GSX2
HMGbox_Sox:like:BHMG1/SOX14/SOX21:lik...
HLH:like:ASCL1/ASCL2:likeclu:45
Homeodomains:POU_POU4F1/POU_POU4F2/PO...
Synaptotagmin:MCTP1/MCTP2
Runt_Runx:RUNX1/RUNX2/RUNX3
bZIP:like:ATF3/JDP2:likeclu:23
HMGbox_Sox:SOX11/SOX12/SOX4
Homeodomains:PRD_PAX2/PRD_PAX5/PRD_PAX8
bZIP:CREBZF
Homeodomains:CERS_CERS2/CERS_CERS3/CE...
HSF:HSF1/HSF2/HSF4
Doublesex_DM:like:DMRT1/DMRT3/DMRTA1/...
bZIP:JUN/JUNB/JUND
Actin, cytoplasmic 2
HLH:HELT
bZIP:like:MAF/MAFA/MAFB/MAFF/MAFG/MAF...
Ets:ETV6/ETV7
bZIP.Unclassified
bZIP:like:MAF/MAFA/MAFB/MAFF/MAFG/MAF...
IRF:IRF1/IRF2
bZIP:CREB3L1/CREB3L2
bZIP:FOS/FOSB/FOSL1/FOSL2
zf−C2H2.Unclassified
HLH:like:HES1/HES2/HES3/HES4/HES5/HES...
Ets:like:AC020909/EHF/ELF1/ELF2/ELF3/...
Forkhead:NA
Adhesion G protein−coupled receptor L2
HLH:like:MYF5/MYF6/MYOD1/MYOG:likeclu:12
Homeodomains:like:PRD_PITX1/PRD_PITX2...
Ets:ERG/FEV/FLI1
HMGbox_Sox:like:SSRP1:likeclu:17
RFX:RFX4/RFX6/RFX8
rRNA−processing protein UTP23 homolog
Forkhead:FOXA1/FOXA2/FOXA3
Homeodomains:like:ANTP_MSX1/ANTP_MSX2...
bZIP:CEBPA/CEBPB/CEBPD/CEBPE/CEBPG
Homeodomains:PRD_ARX
Homeodomains:like:PRD_PITX1/PRD_PITX2...
cDNA FLJ56616, highly similar to Sema...
Homeodomains:like:ANTP_NKX2−1/ANTP_NK...
HCG15971
Homeodomains:ANTP_DBX1/ANTP_DBX2/ANTP...
HLH:ID1/ID2/ID3/ID4
Homeodomains:ANTP_BARX1/ANTP_BARX2
Alpha−2 macroglobulin receptor
Prolow−density lipoprotein receptor−r...
Homeodomains:PRD_CRX/PRD_OTX1/PRD_OTX2
bZIP:like:DBP/HLF/NFIL3/TEF:likeclu:1...
Homeodomains:PRD_DMBX1
Collagen:like:COL1A1/COL1A2/COL2A1/CO...
Collagen:like:COL1A1/COL1A2/COL2A1/CO...
T−box:TBX1/TBX10
HLH:like:SCX/TCF15:likeclu:34
Transgelin−2
Homeodomains:ANTP_MEOX1/ANTP_MEOX2
Ferritin
Ferritin
Hemicentin−1
Homeodomains:ANTP_HOXA2/ANTP_HOXA3/AN...
E2F_TDP:E2F4/E2F5
cDNA FLJ16032 fis, clone NTONG2003316...
Ferritin
Epididymis secretory protein Li 108
MYL9 protein
Myosin, light polypeptide 6B, alkali,...
HCG15971
HLH:like:SCX/TCF15:likeclu:34
Collagen:NA
bZIP:JUN/JUNB/JUND
zf−met:NA
Forkhead:FOXL2

C

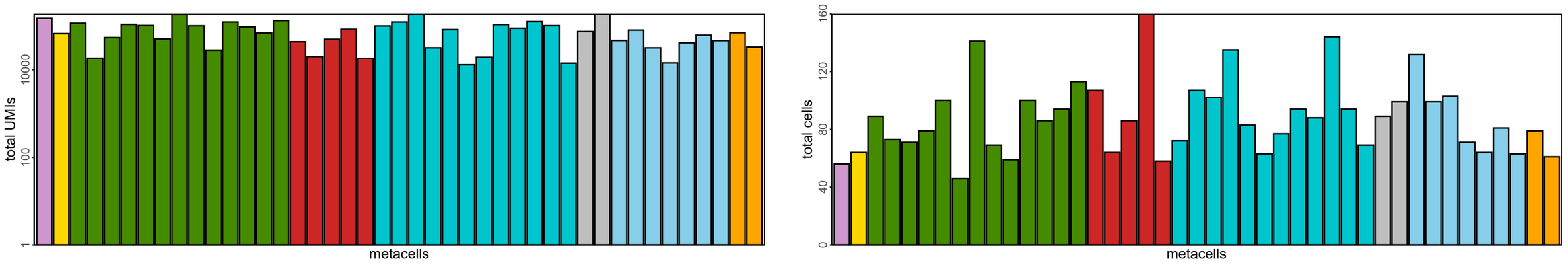
total UMIs
10000
100
1
metacells
total cells
160
120
80
40
0
metacells

A

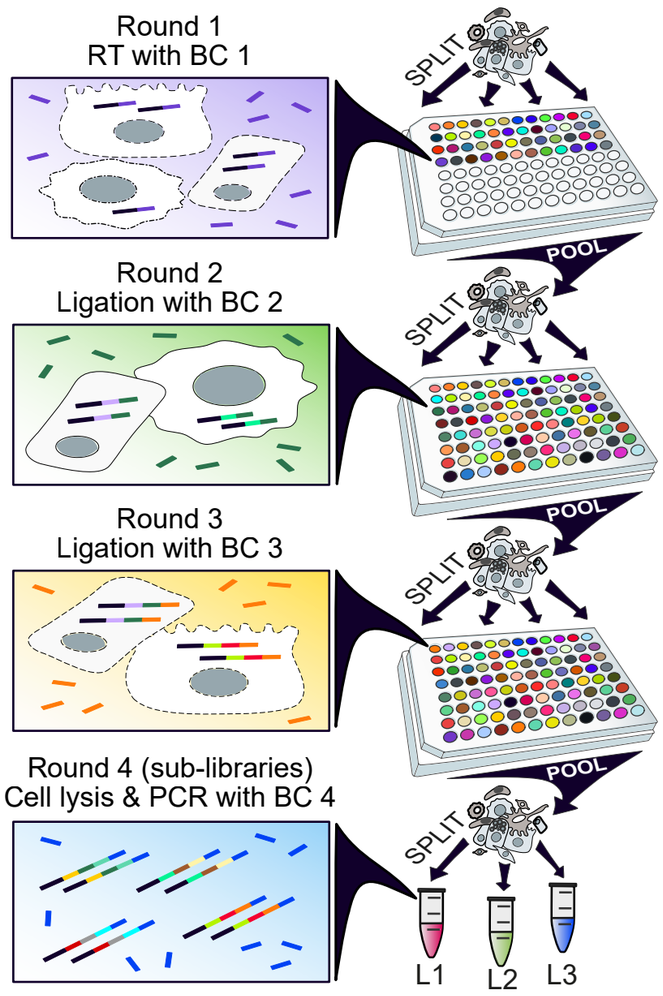
Round 1
RT with BC 1
SPLIT
POOL
Round 2
Ligation with BC 2
SPLIT
POOL
Round 3
Ligation with BC 3
SPLIT
POOL
Round 4 (sub-libraries)
Cell lysis & PCR with BC 4
SPLIT
L1
L2
L3

B

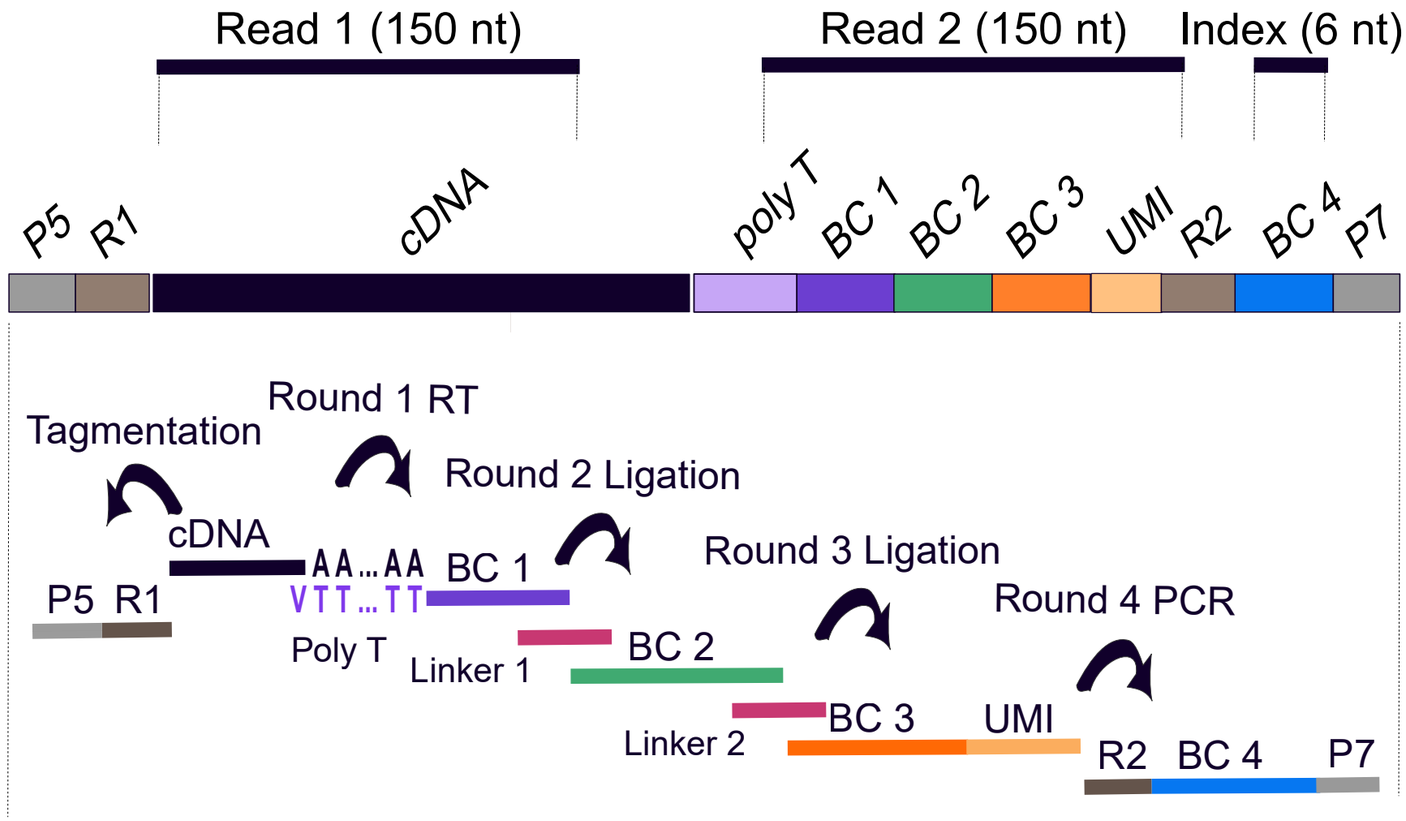
Read 1 (150 nt)
Read 2 (150 nt)
Index (6 nt)
P5
R1
cDNA
poly T
BC 1
BC 2
BC 3
UMI
R2
BC 4
P7
Tagmentation
Round 1 RT
Round 2 Ligation
Round 3 Ligation
Round 4 PCR
cDNA
AA...AA
VTT...TT
BC 1
P5
R1
Poly T
Linker 1
BC 2
Linker 2
BC 3
UMI
R2
BC 4
P7

C

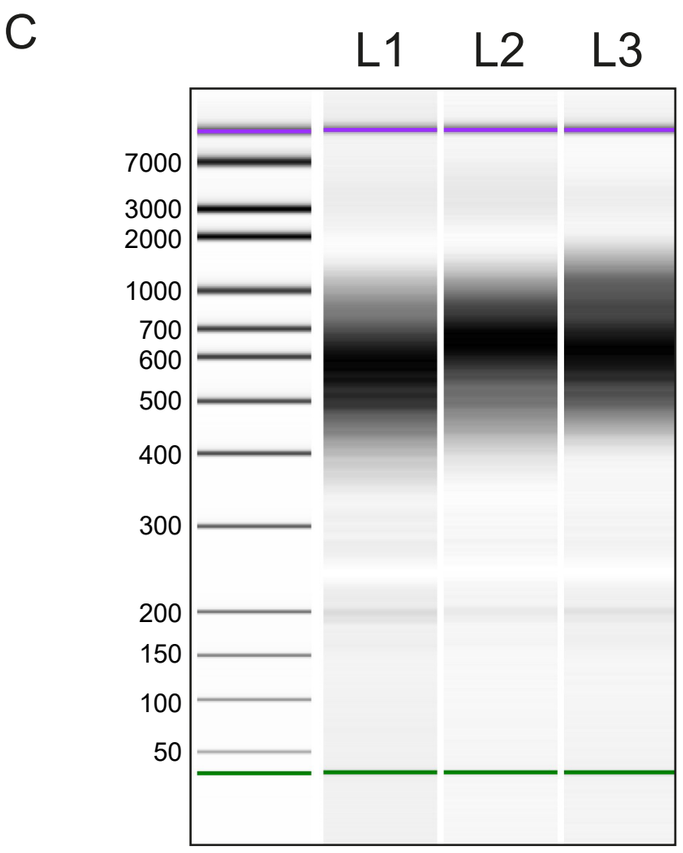
L1
L2
L3
7000
3000
2000
1000
700
600
500
400
300
200
150
100
50

D

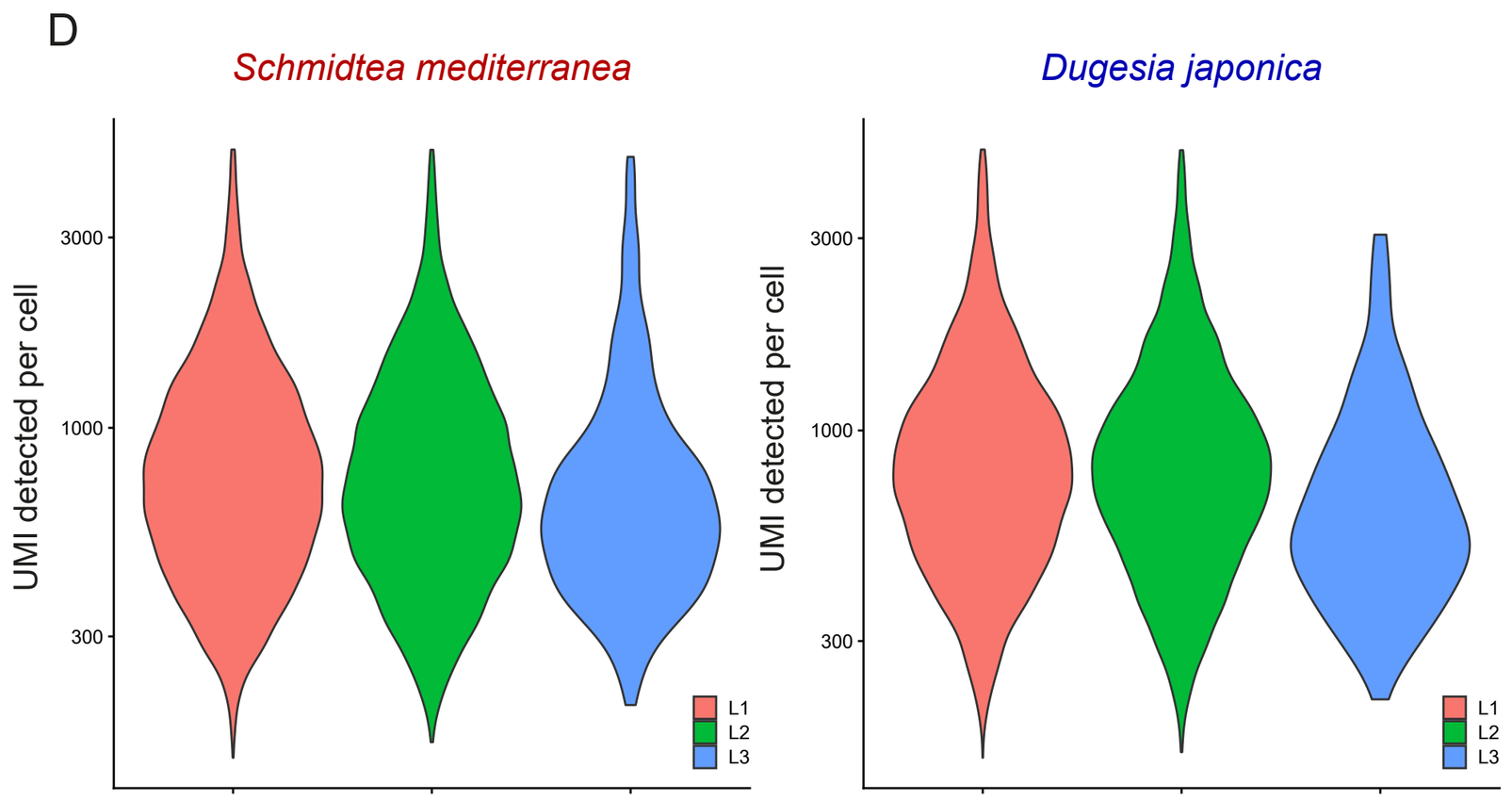
Schmidtea mediterranea
Dugesia japonica
UMI detected per cell
3000
1000
300
L1
L2
L3

E

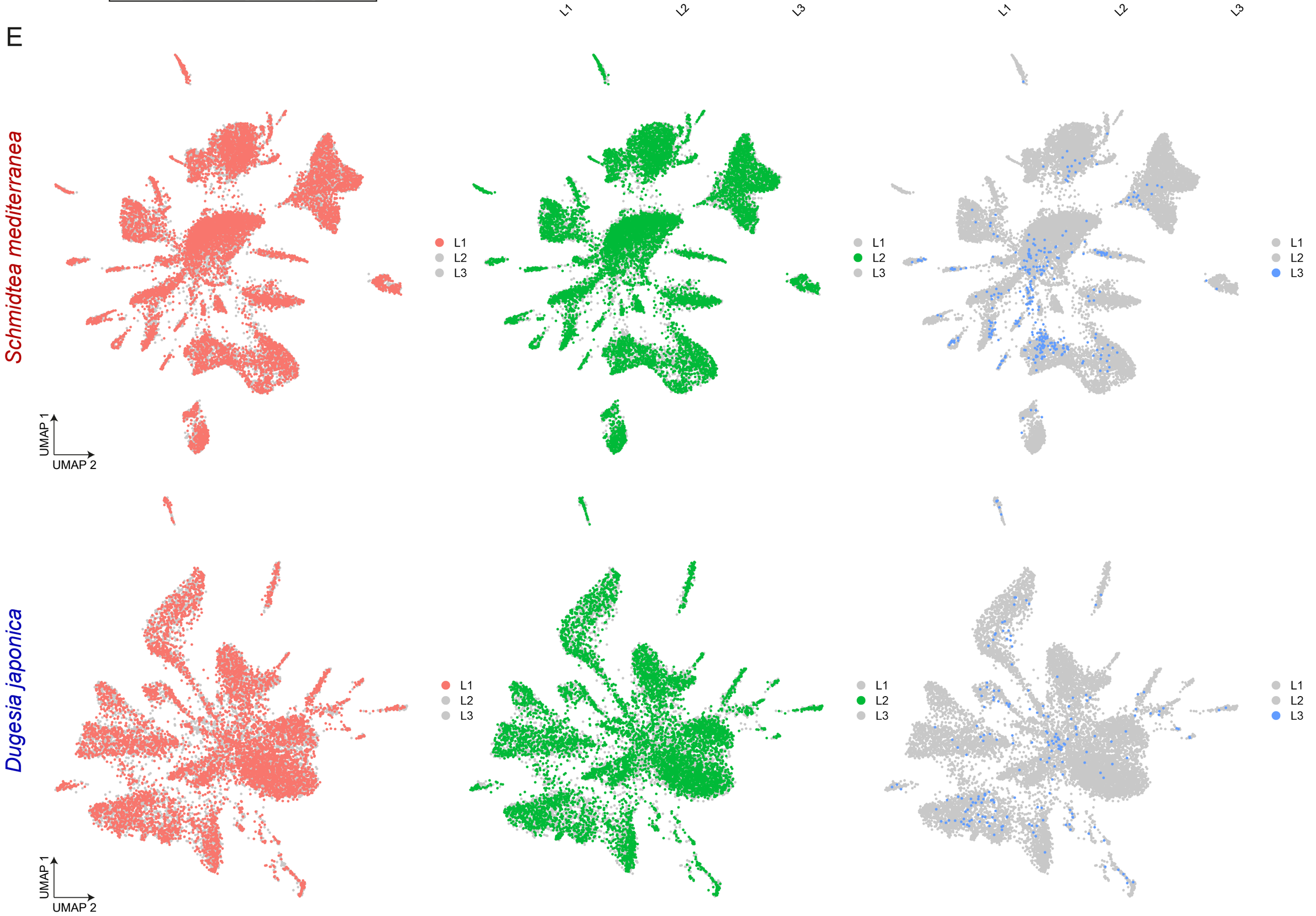
Schmidtea mediterranea
Dugesia japonica
L1
L2
L3
UMAP 1
UMAP 2

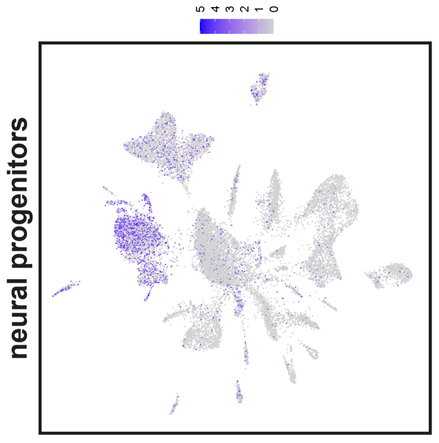
neural progenitors
dd_Smed_v6_2164_0/SmMSTRG.6422

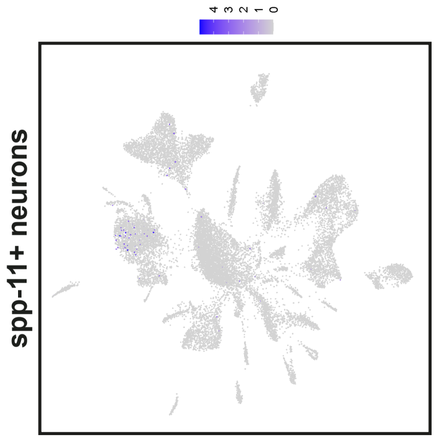
spp-11+ neurons
dd_Smed_v6_1737_0/SmMSTRG.2535

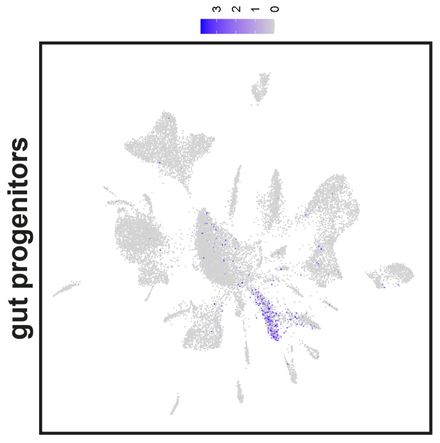
gut progenitors
dd_Smed_v6_1144_0/SmMSTRG.12889

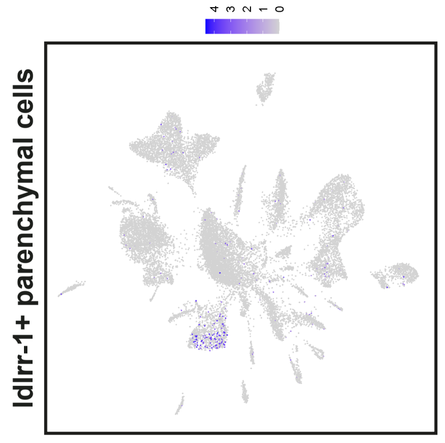
ldlrr-1+ parenchymal cells
dd_Smed_v6_74_0/SmMSTRG.16779

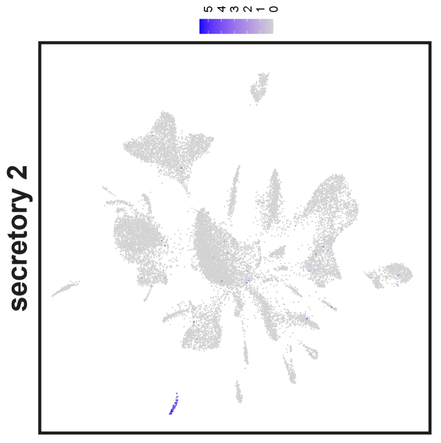
secretory 2
dd_Smed_v6_518_0/SmMSTRG.4346

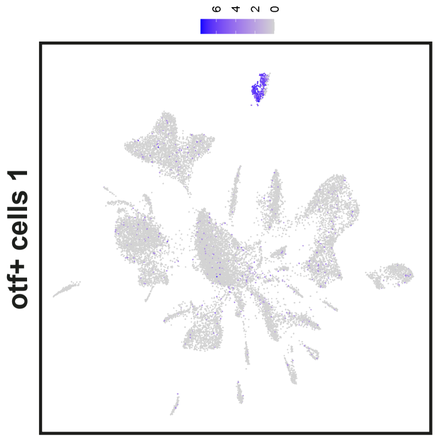
otf+ cells 1
dd_Smed_v6_1248_0/SmMSTRG.21121

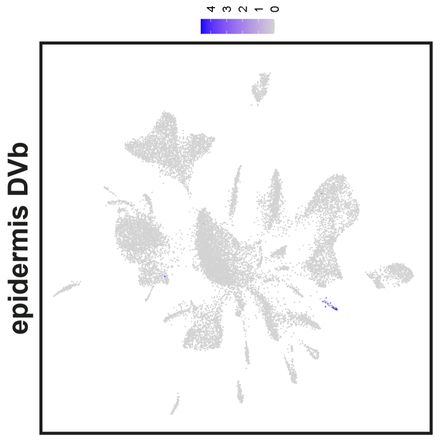
epidermis DVb
dd_Smed_v6_3199_0/SmMSTRG.10597

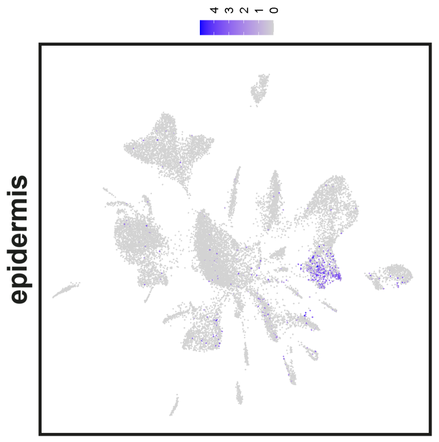
epidermis
dd_Smed_v6_181_0/SmMSTRG.11769

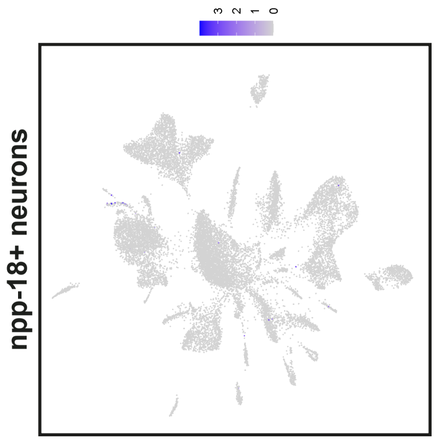
npp-18+ neurons
dd_Smed_v6_14386_0/SmMSTRG.21557

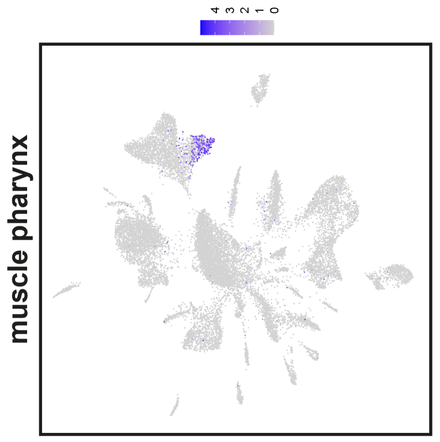
muscle pharynx
dd_Smed_v6_8356_0/SmMSTRG.22296

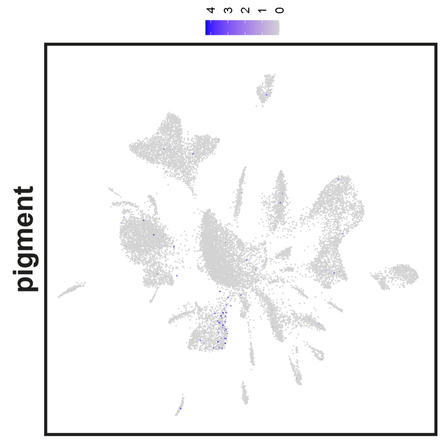
pigment
dd_Smed_v6_873_0/SmMSTRG.6149

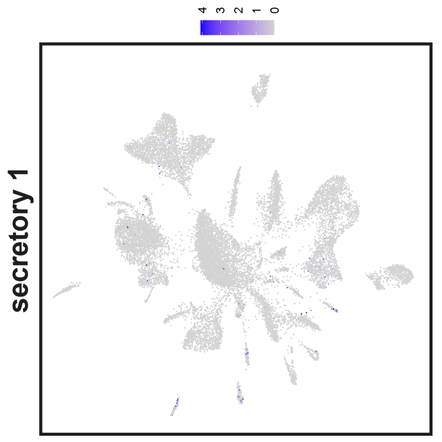
secretory 1
dd_Smed_v6_854_1/SmMSTRG.15146

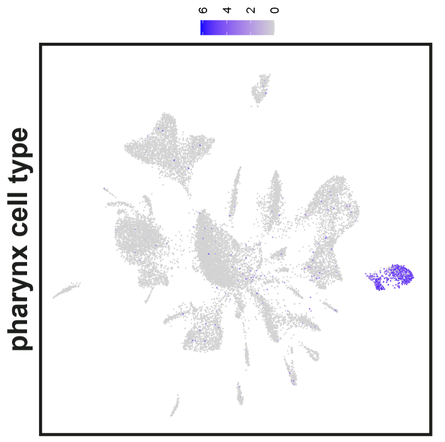
pharynx cell type
dd_Smed_v6_1071_0/SmMSTRG.10563

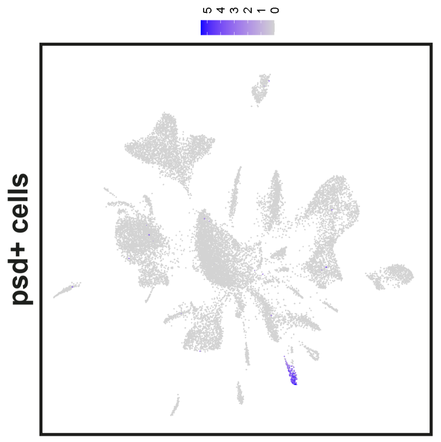
psd+ cells
dd_Smed_v6_531_0/SmMSTRG.19456

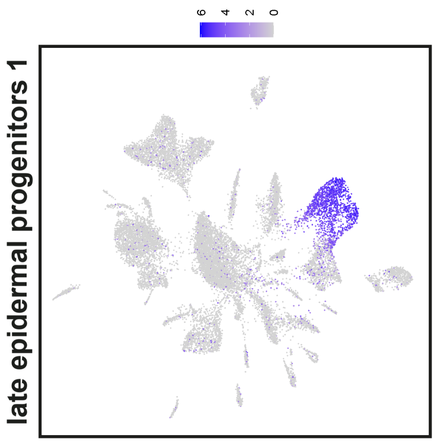
late epidermal progenitors 1
dd_Smed_v6_2178_0/SmMSTRG.20313

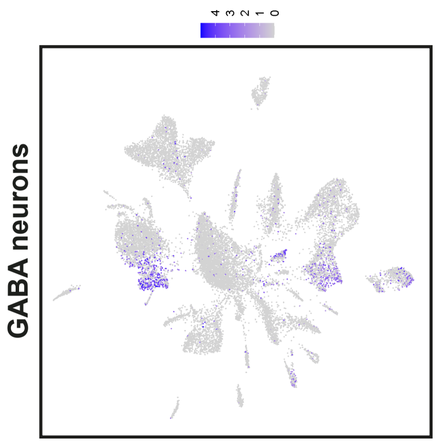
GABA neurons
dd_Smed_v6_6573_0/SmMSTRG.22759

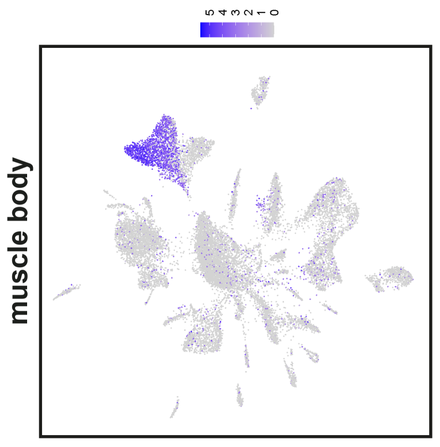
muscle body
dd_Smed_v6_432_0/SmMSTRG.17020

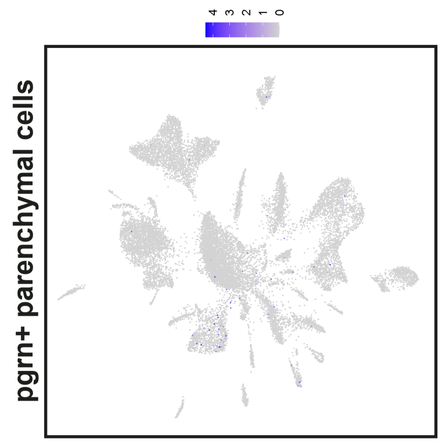
pgrn+ parenchymal cells
dd_Smed_v6_780_0/SmMSTRG.852

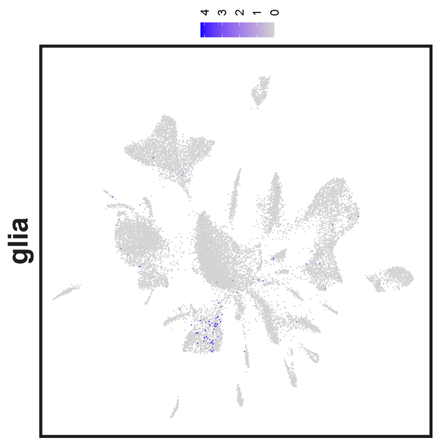
glia
dd_Smed_v6_1170_0/SmMSTRG.2961

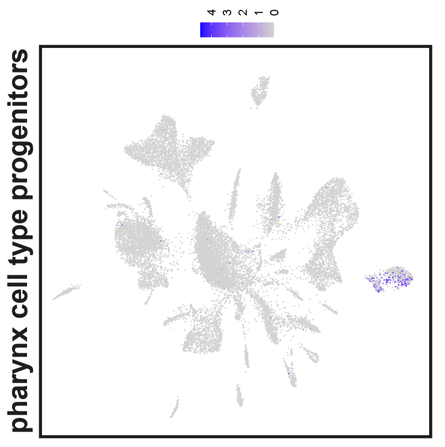
pharynx cell type progenitors
dd_Smed_v6_561_0/SmMSTRG.9564

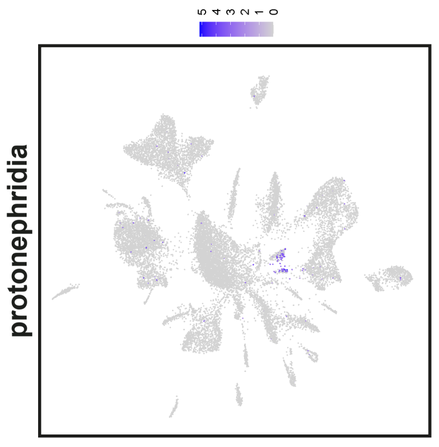
protonephridia
dd_Smed_v6_5233_0/SmMSTRG.20094

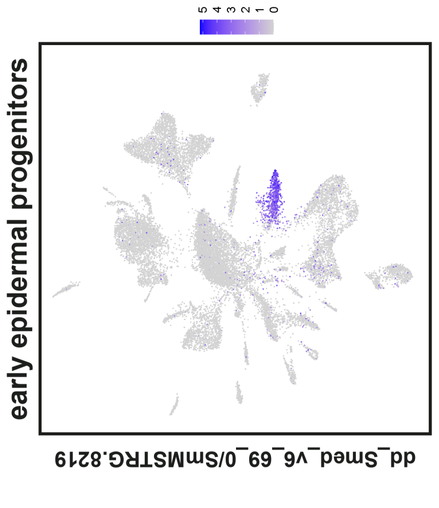
early epidermal progenitors
dd_Smed_v6_69_0/SmMSTRG.8219

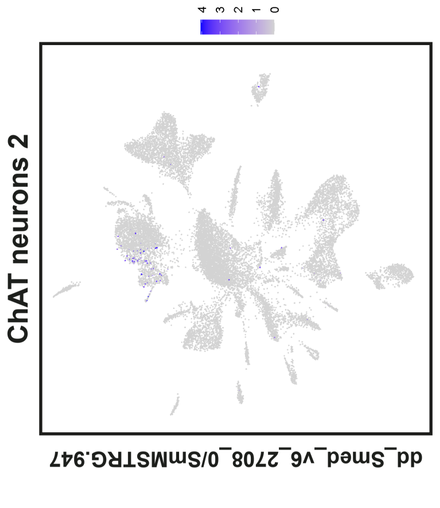
ChAT neurons 2
dd_Smed_v6_2708_0/SmMSTRG.947

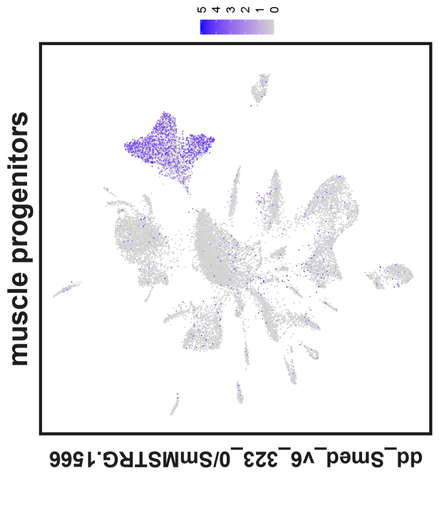
muscle progenitors
dd_Smed_v6_323_0/SmMSTRG.1566

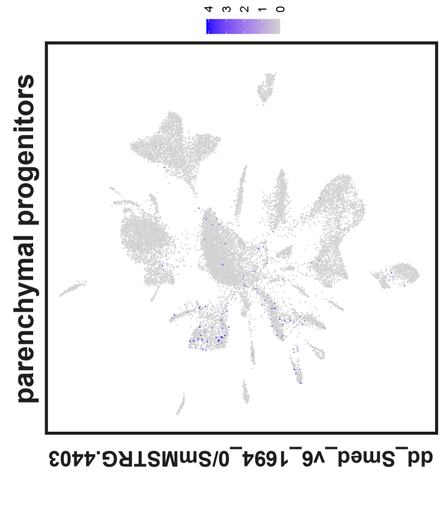
parenchymal progenitors
dd_Smed_v6_1694_0/SmMSTRG.4403

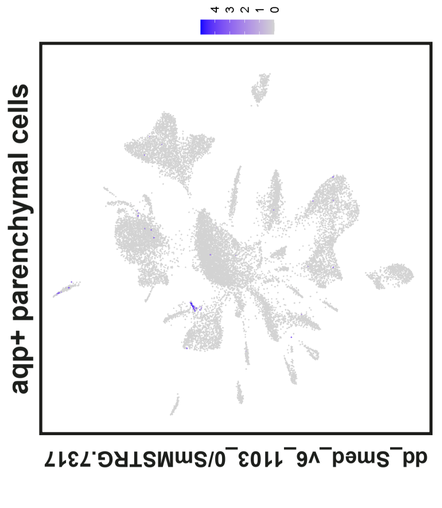
aqp+ parenchymal cells
dd_Smed_v6_1103_0/SmMSTRG.7317

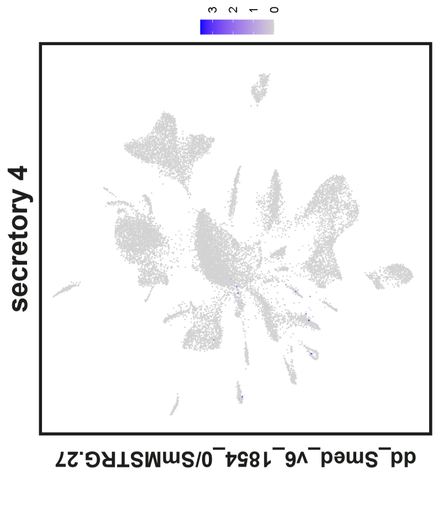
secretory 4
dd_Smed_v6_1854_0/SmMSTRG.27

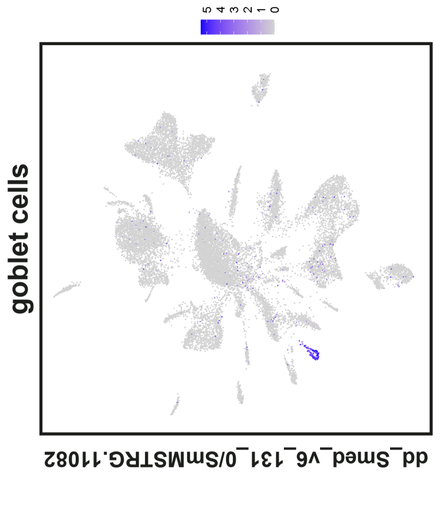
goblet cells
dd_Smed_v6_131_0/SmMSTRG.11082

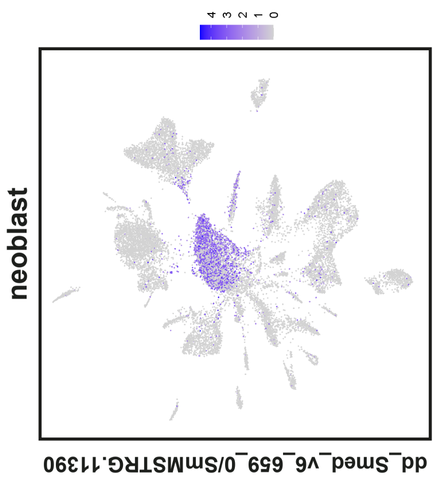
neoblast
dd_Smed_v6_659_0/SmMSTRG.11390

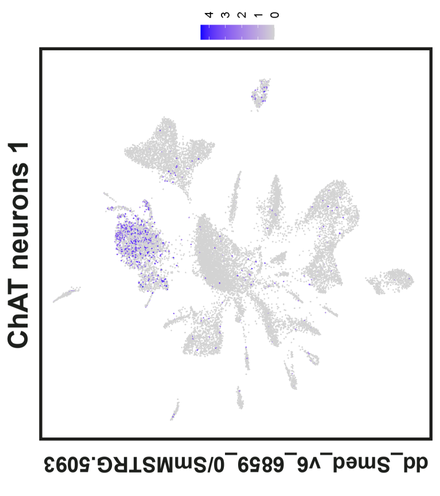
ChAT neurons 1
dd_Smed_v6_6859_0/SmMSTRG.5093

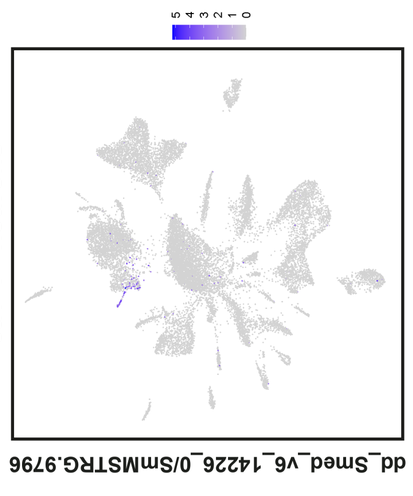
cav-1+ neurons
dd_Smed_v6_14226_0/SmMSTRG.9796

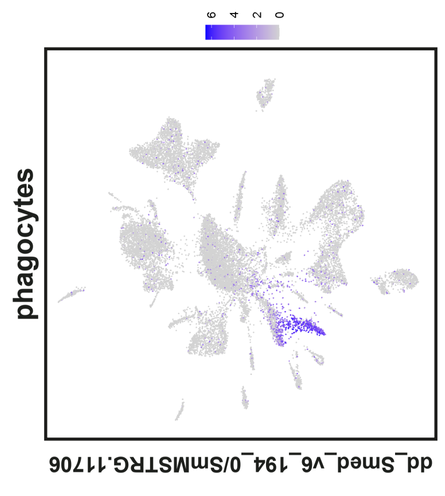
phagocytes
dd_Smed_v6_194_0/SmMSTRG.11706

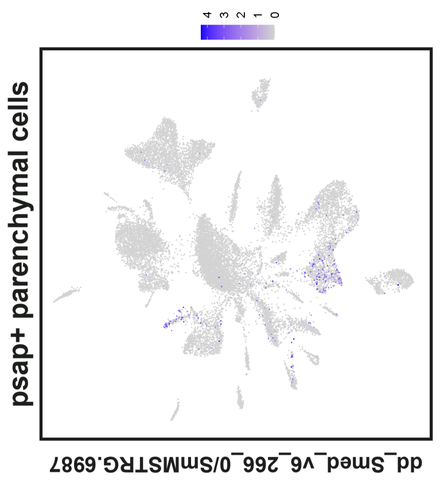
psap+ parenchymal cells
dd_Smed_v6_266_0/SmMSTRG.6987

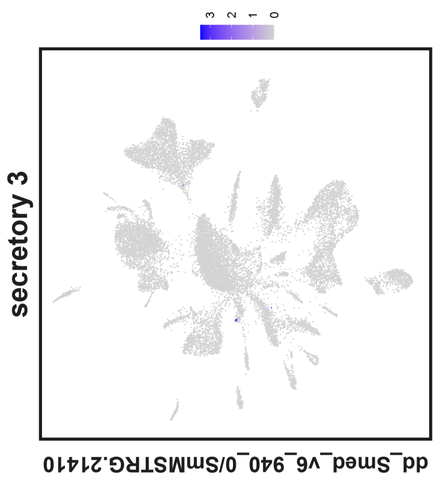
secretory 3
dd_Smed_v6_940_0/SmMSTRG.21410

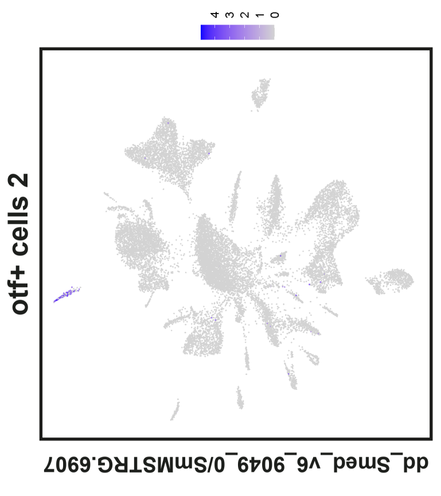
otf+ cells 2
dd_Smed_v6_9049_0/SmMSTRG.6907

A

Schmidtea mediterranea

This study

***Smed-eIF3c* (HM055595)**

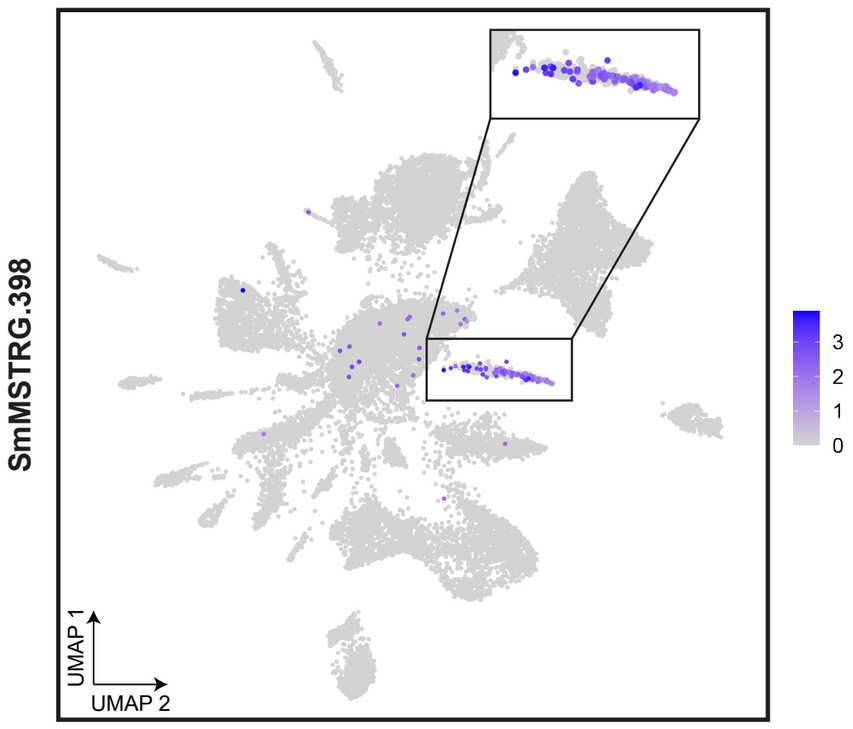

***Smed-nanos* (EF035555)**

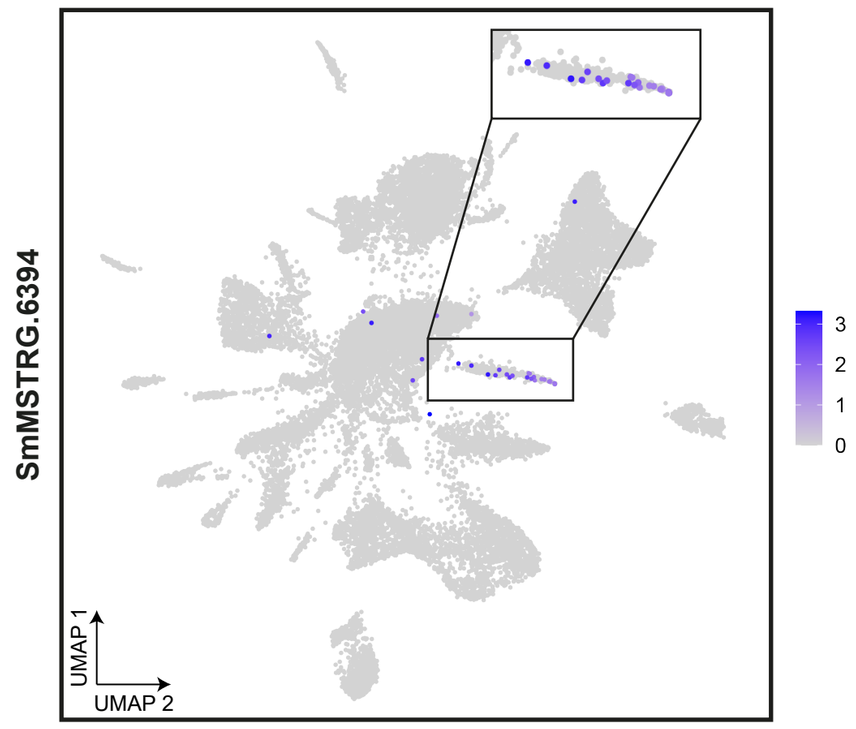

Plass *et al*.

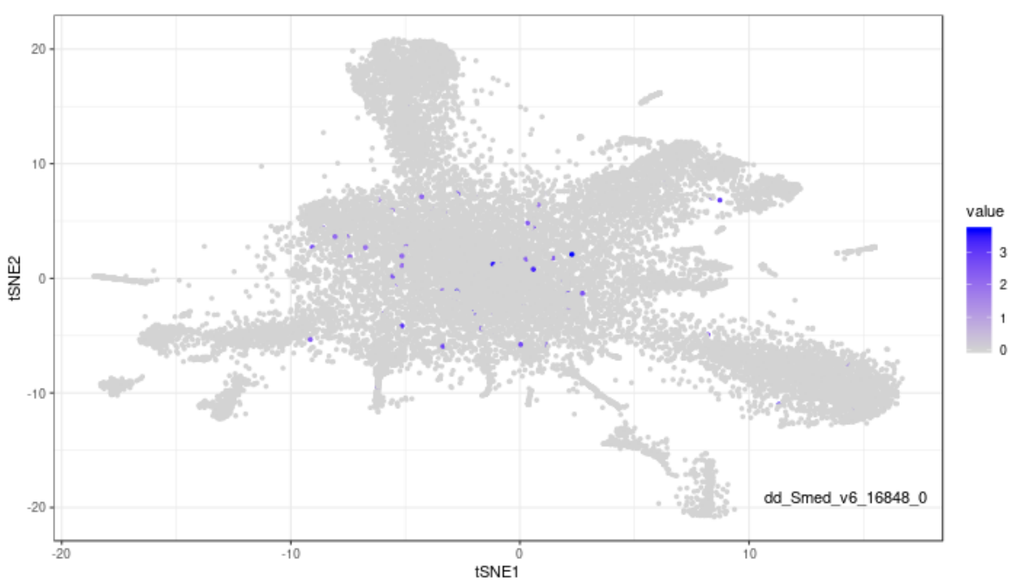

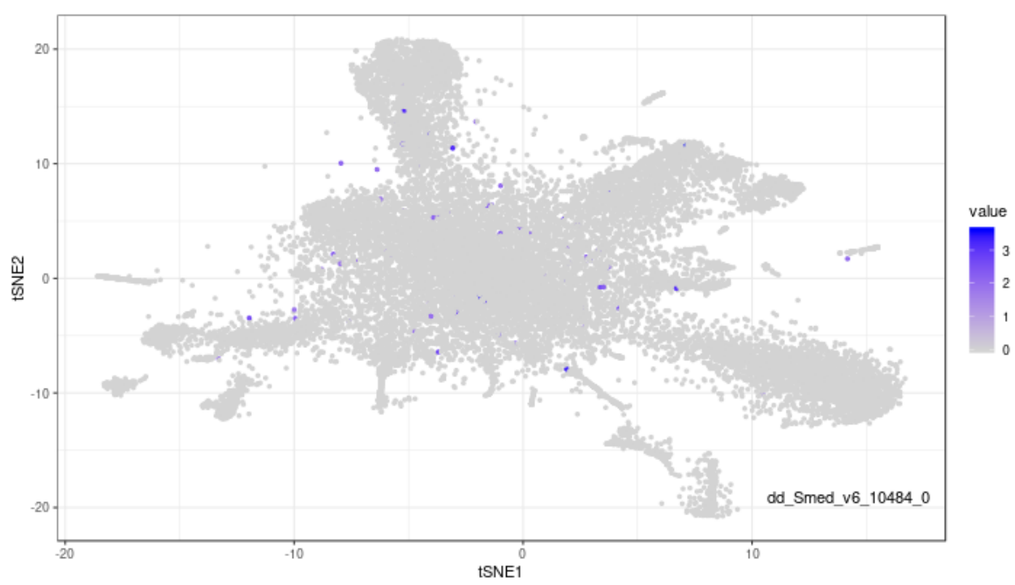

Fincher *et al*.

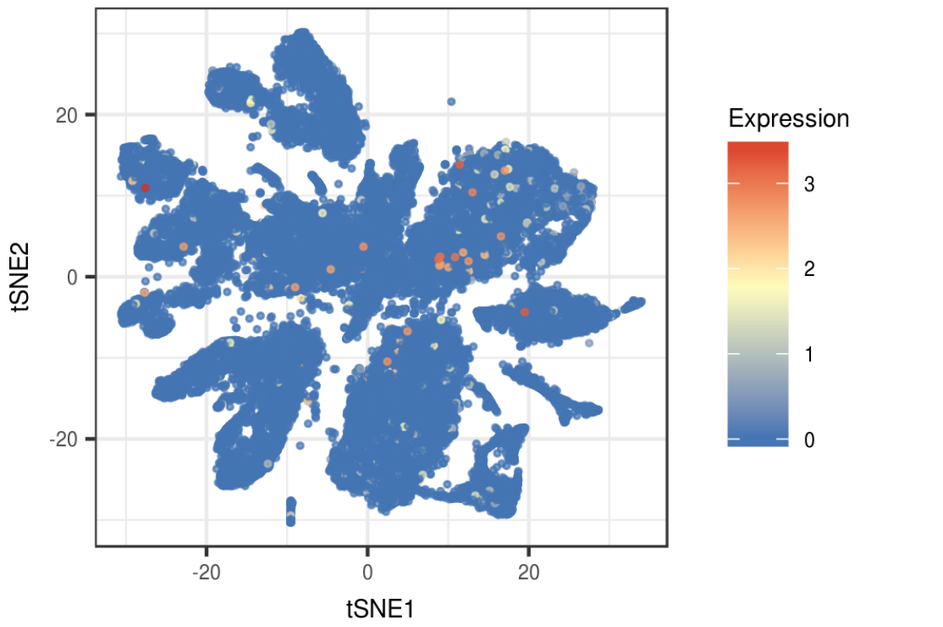

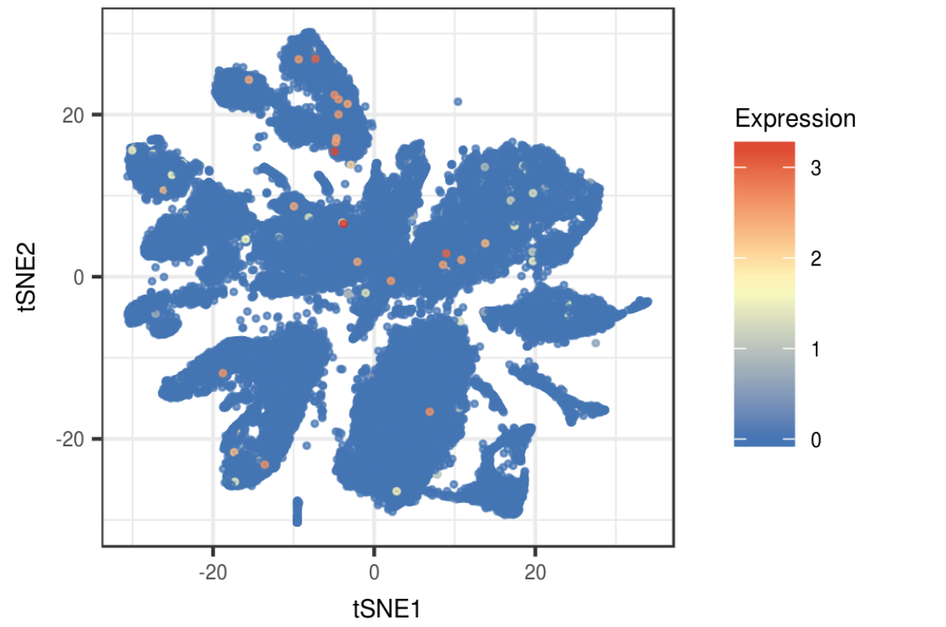

Zeng *et al*.

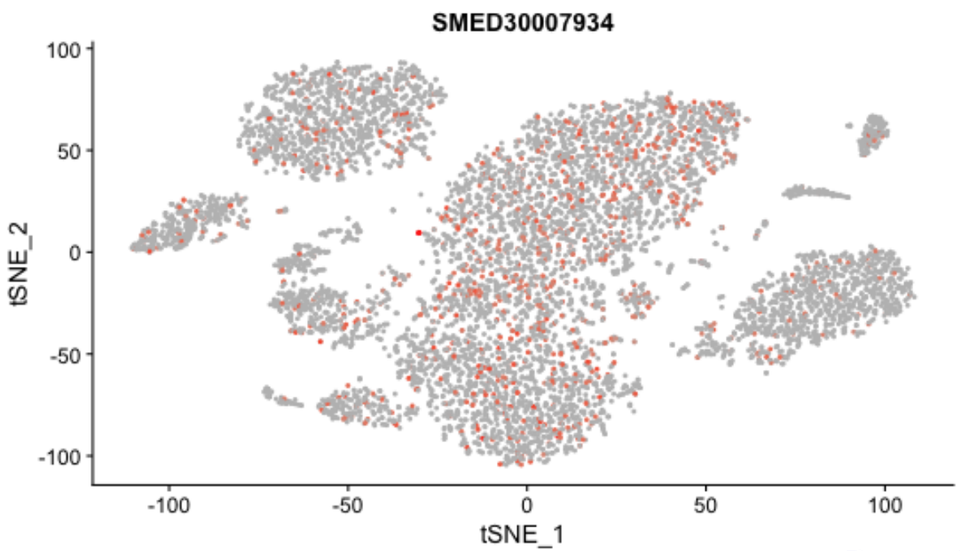

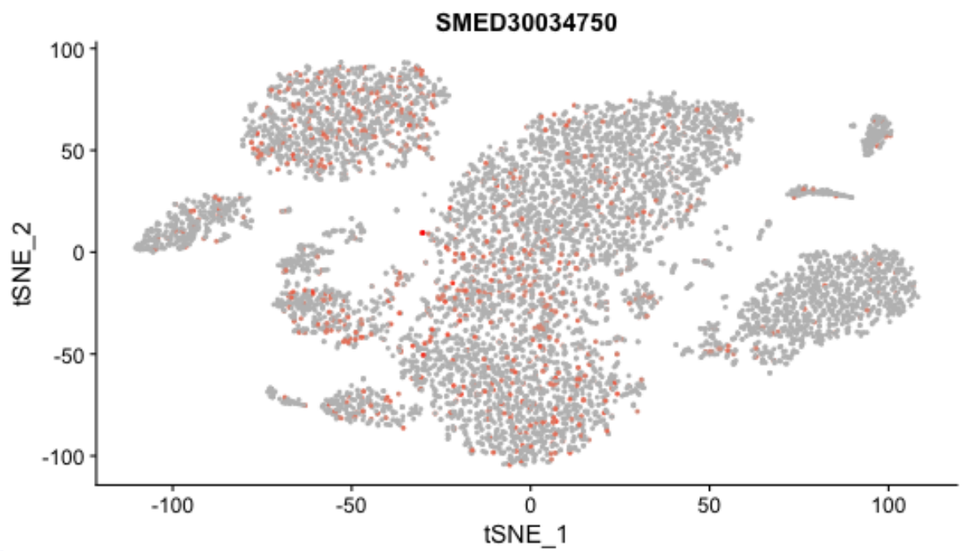

B

Dugesia japonica

This study

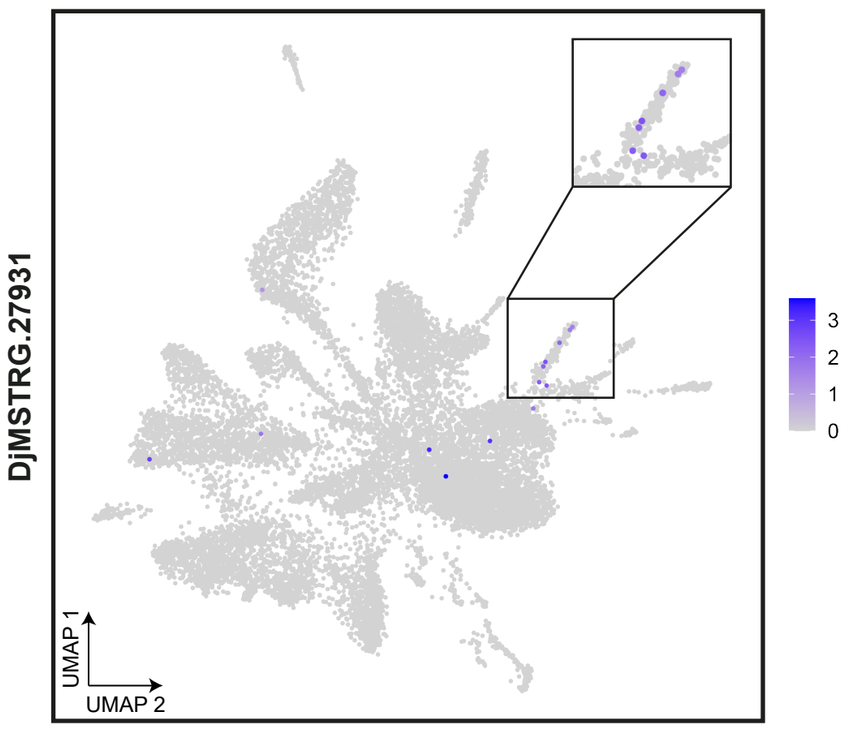

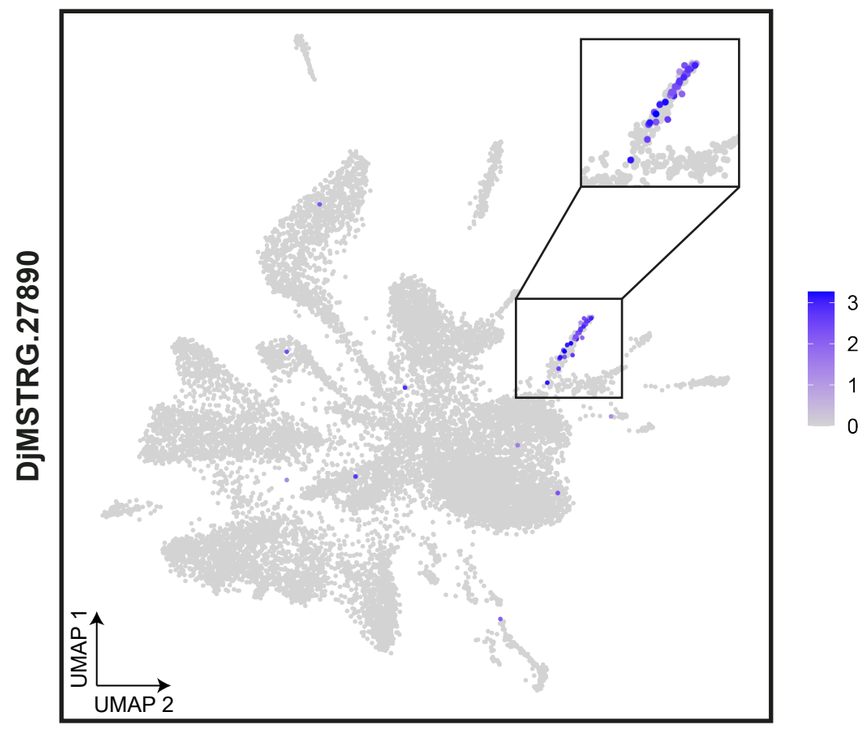

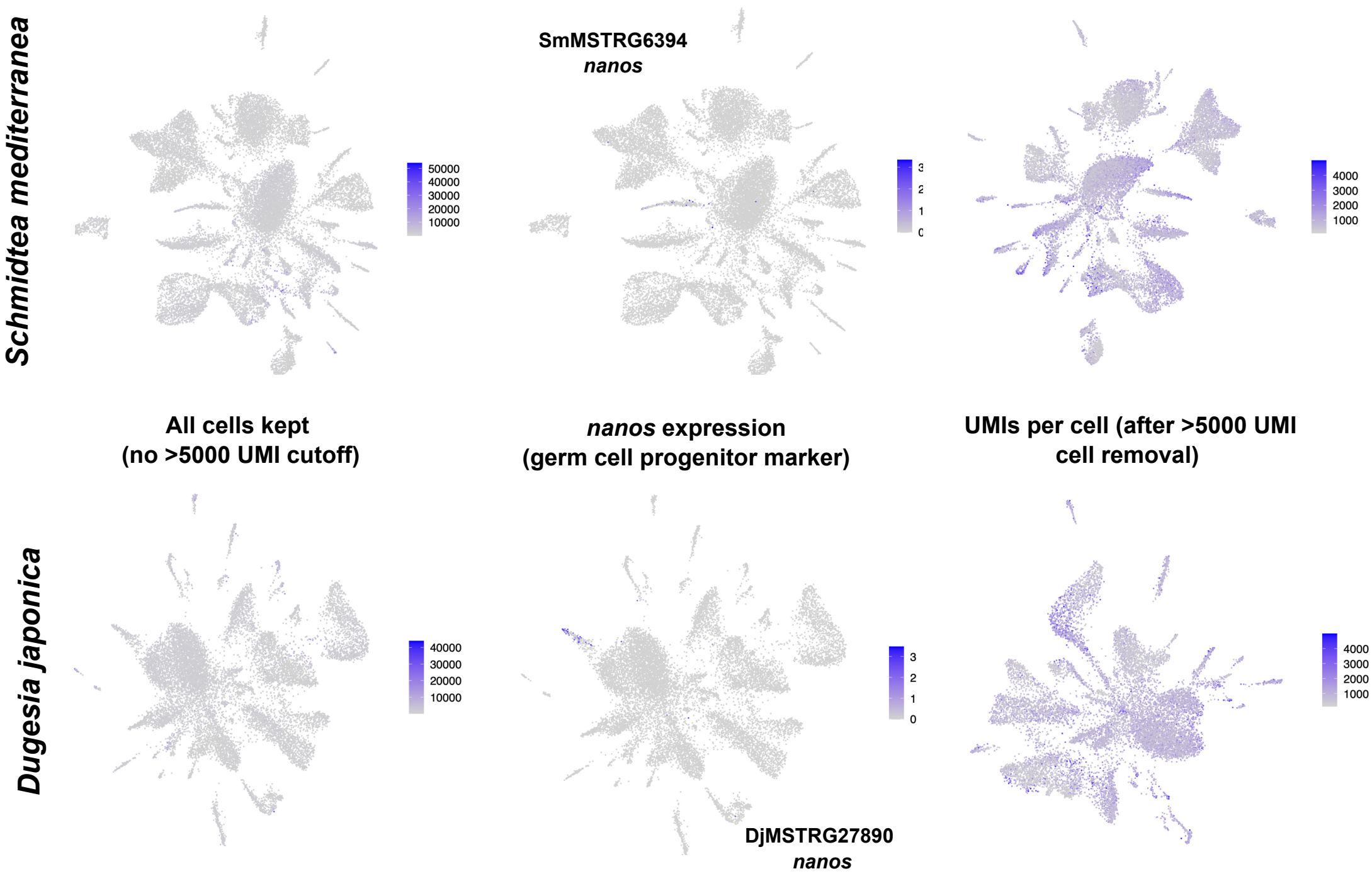
Schmidtea mediterranea
SmMSTRG6394
nanos
50000
40000
30000
20000
10000
4000
3000
2000
1000
All cells kept
(no >5000 UMI cutoff)
nanos expression
(germ cell progenitor marker)
UMIs per cell (after >5000 UMI
cell removal)
Dugesia japonica
40000
30000
20000
10000
3
2
1
0
4000
3000
2000
1000
DjMSTRG27890
nanos

Statistics on UMI and gene count:

	Plass et al (this reanalysis)	García-Castro et al (this dataset)
All reads	1,200,007,715	1,362,741,948
Usable reads	1,200,007,715	560,518,316
Mapped reads (to genome)	399,074,916	470,671,761
Mapped reads (to genes)	343,409,649	427,296,897
Mapped reads (intronic content)	81,299,126	161,656,944
Total cells	21,610	32,431
Total UMIs	21,288,321	29,557,182
Total genes	12,233,806	6,837,300
Statistics for each sample (nb in García-Castro, 2 species combined)		
UMIs per cell (mean)	985.1	911.4
Genes per cell (mean)	566.1	210.8
UMIs per cell (median)	696	741
Genes per cell (median)	452	179
UMI per million raw reads	17,740.2	21,689.5
Genes per million raw reads	10,194.8	5,017.3
UMI per million usable reads	17,740.2	52,731.9
Genes per million usable reads	10,194.8	12,198.2
Statistics after downsampling <u>all</u> García-Castro reads to 1,200,007,715 (Plass total)		
UMIs	21,288,321	27,939,680
Genes	12,233,806	6,581,986
UMIs per cell (mean)	939.8	861.5
Genes per cell (mean)	541.8	203.0
UMIs per cell (median)	696	700
Genes per cell (median)	452	172
UMI per million reads	17,740.2	23,282.9
Genes per million reads	10,194.8	5,485.0
Statistics after downsampling both to 10k <u>mapped</u> reads per cell		
Mapped Reads	216,100,000	324,310,000
UMIs	17,858,300	28,840,440
Genes	10,569,570	6,719,416
UMIs per cell (mean)	826.4	889.3
Genes per cell (mean)	489.1	207.2
UMIs per cell (median)	594	723
Genes per cell (median)	394	176
UMI per million reads	82,639.1	88,928.6
Genes per million reads	48,910.6	20,719.1

García-Castro downsampled to Plass Total

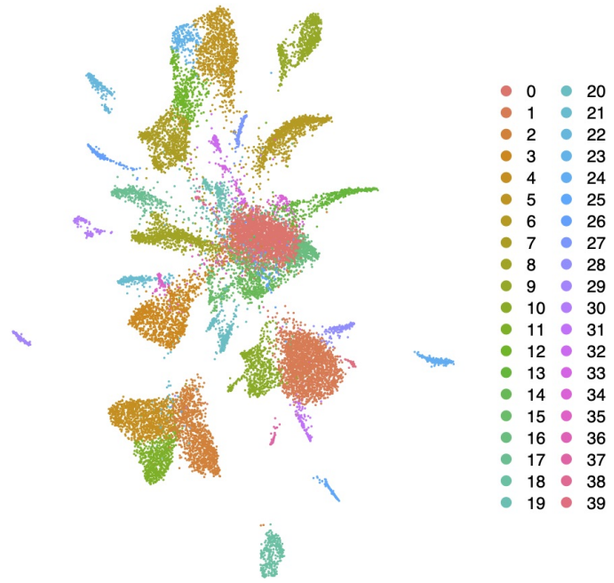

García-Castro Downsampeld to 10k Per Cell

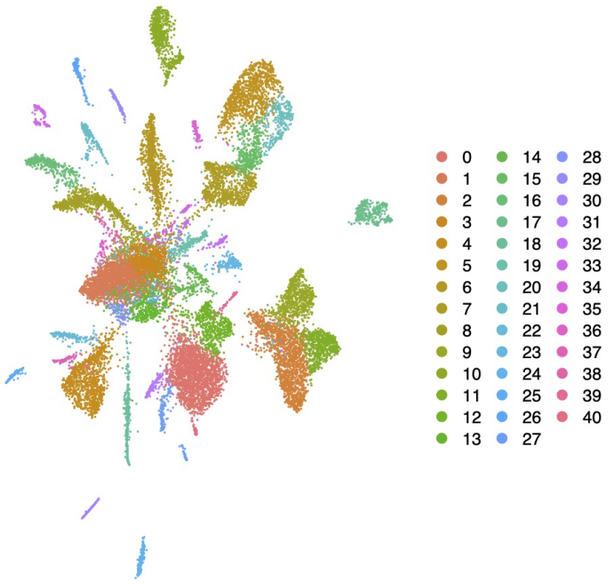

Plass downsampled to 10k Mapped Per Cell

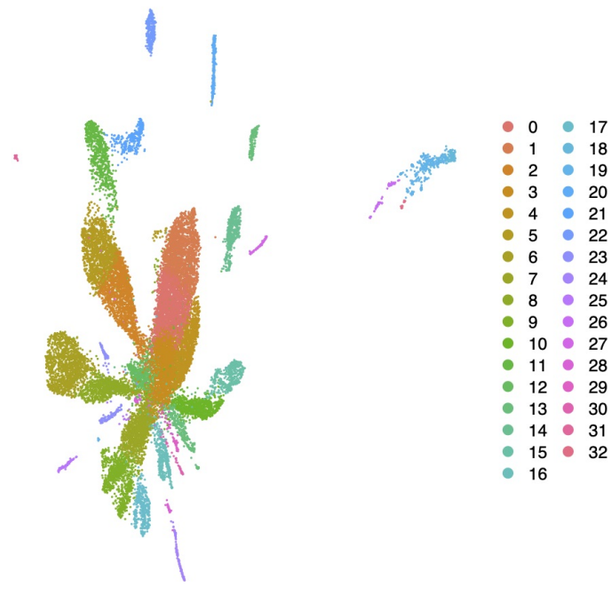

	Number of genes differentially expressed in ACME-dissociated dataset	Number of overlaps with Trypsin dissociated dataset (Plass et al)	Percentage overlap	Neoblast cluster numbers (ACME-dissociated dataset, Garcia-Castro)	Test clusters (ACME-dissociated dataset, Garcia-Castro et al)	Neoblast cluster numbers (Trypsin dissociated dataset, Plass et al)	Test clusters (Trypsin dissociated dataset, Plass et al)
Neoblast vs GABA neuron	333	281	84.4	1, 2, 15, 17, 40	10	0, 1, 4, 6, 12, 17, 25, 33	16
Neoblast vs differentiated Goblet	365	304	83.3	1, 2, 15, 17, 40	32	0, 1, 4, 6, 12, 17, 25, 33	37
Neoblast vs muscle	354	272	76.8	1, 2, 15, 17, 40	3, 6, 11	0, 1, 4, 6, 12, 17, 25, 33	7, 8, 19
Neoblast vs Otf	429	354	82.5	1, 2, 15, 17, 40	16, 21	0, 1, 4, 6, 12, 17, 25, 33	28, 29
Neoblast vs Pharynx	421	313	74.3	1, 2, 15, 17, 40	13, 23	0, 1, 4, 6, 12, 17, 25, 33	26

Differential expression analysis performed in Seurat with FindMarkers, with a Wilcoxon Rank Sum test, logfc.threshold of 0.25, and a min.pct value of 0.1

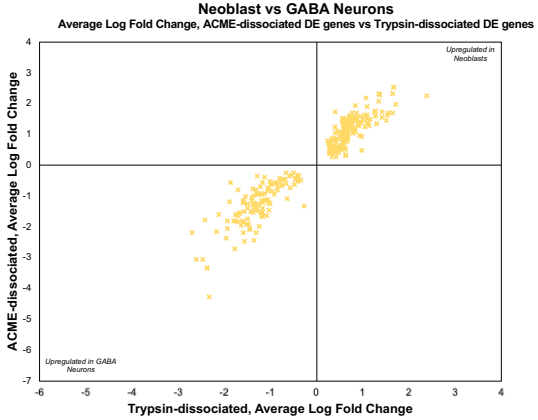

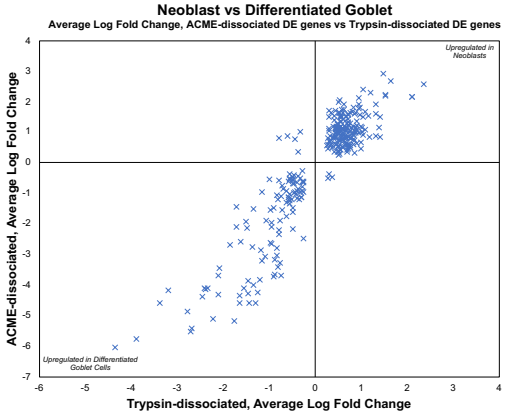

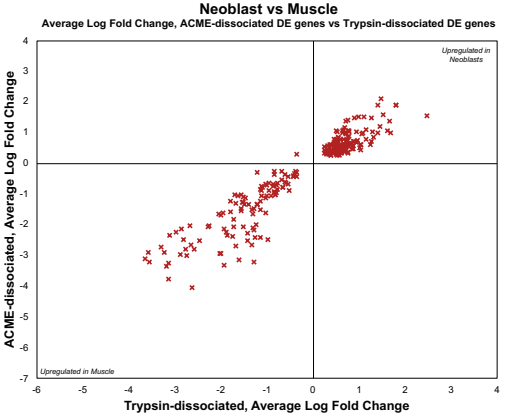

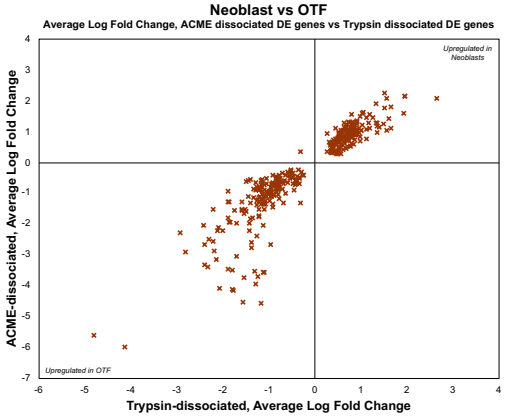

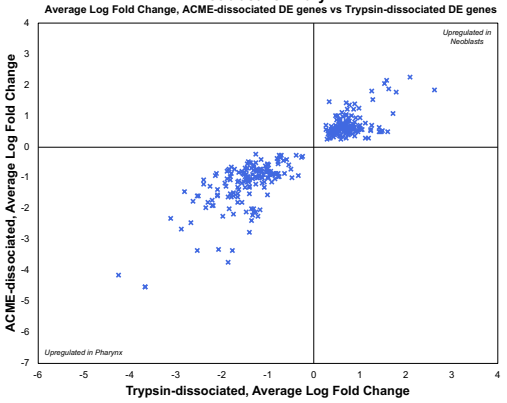

A

This study (19,025 cells)

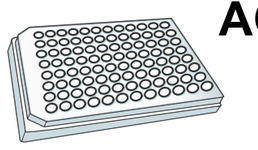

ACME dissociation
+ FACS
+ SPLiT-seq

Plass *et al.* Science 2018 (21,610 cells)

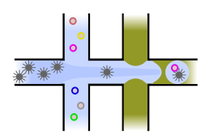

Trypsin dissociation
+ FACS
+ Drop-seq

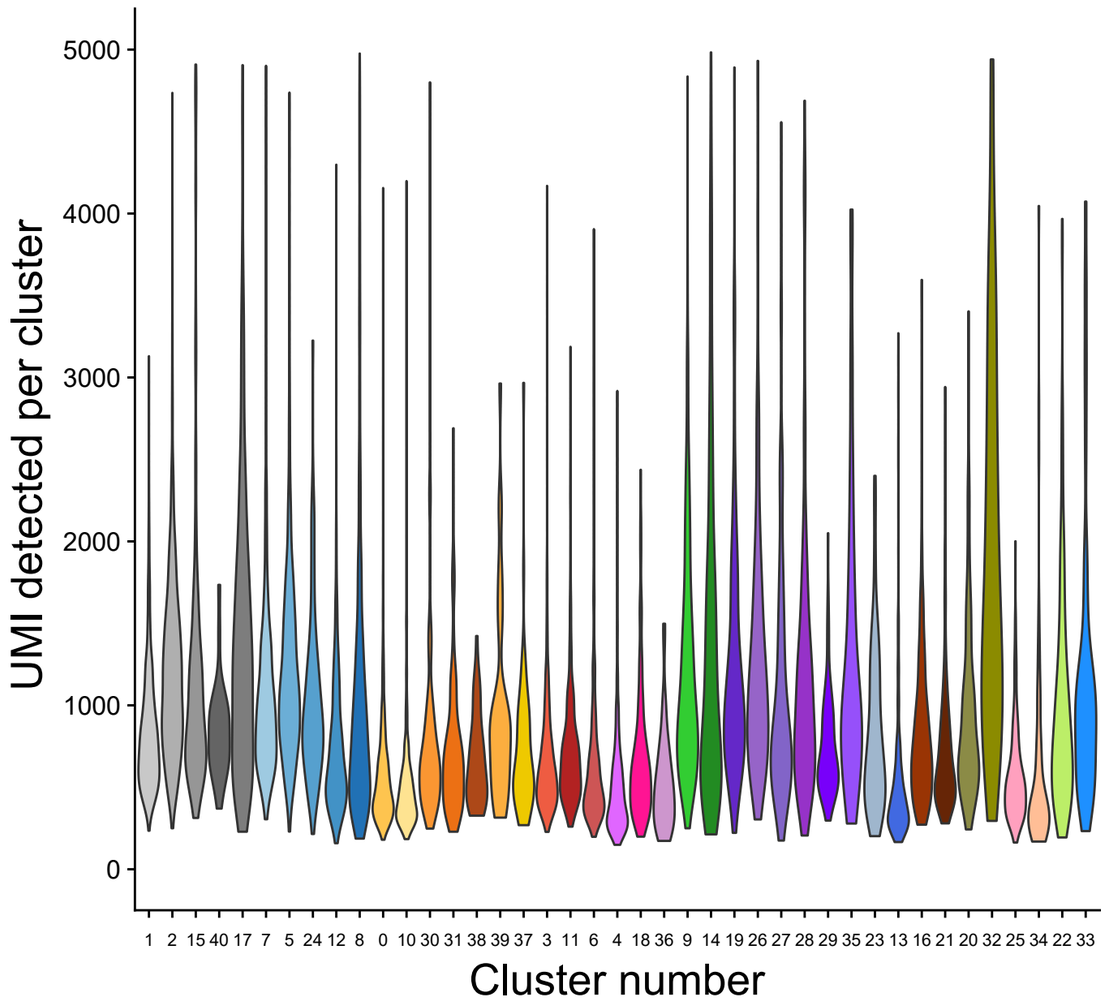

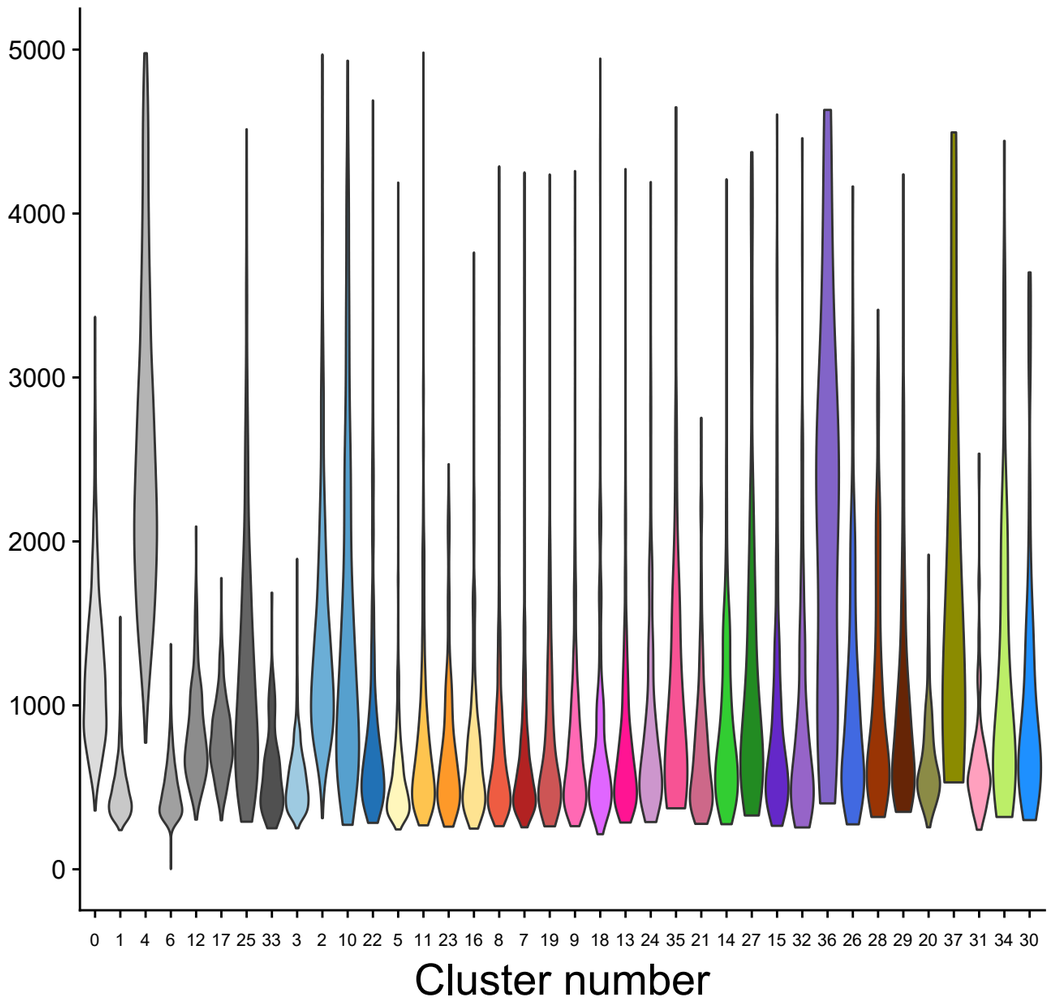

B

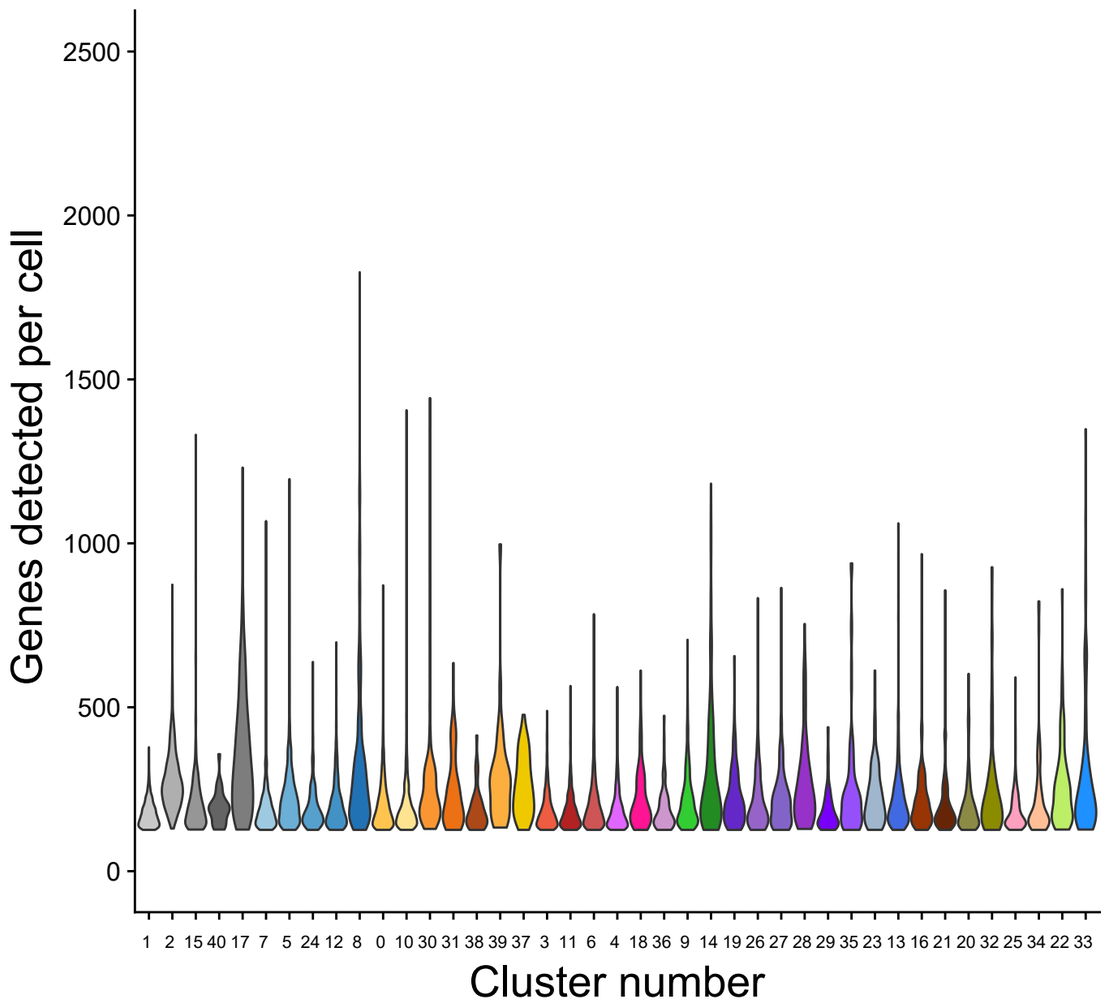

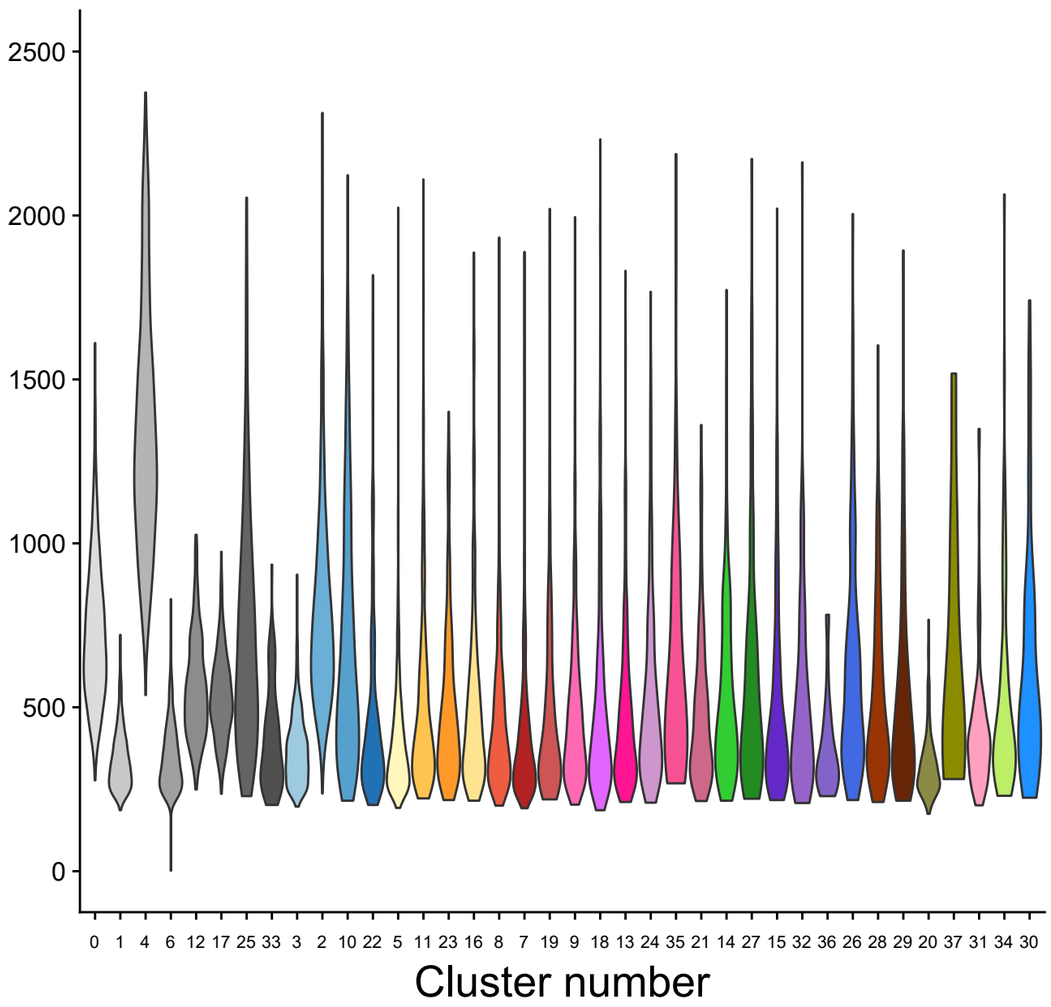

A

Plass *et al*.
Science 2018

This study
(genome
annotation)

Seurat
(Stuart *et al*.
Cell 2019)

This study

Trypsin dissociation
+ FACS
+ Drop-seq

Data re-analysis

Transfer labels

Data Integration

ACME dissociation
+ FACS
+ SPLiT-seq

Panel E

B

Trypsin-dissociated dataset (21,610 cells)
Labels transferred from this study

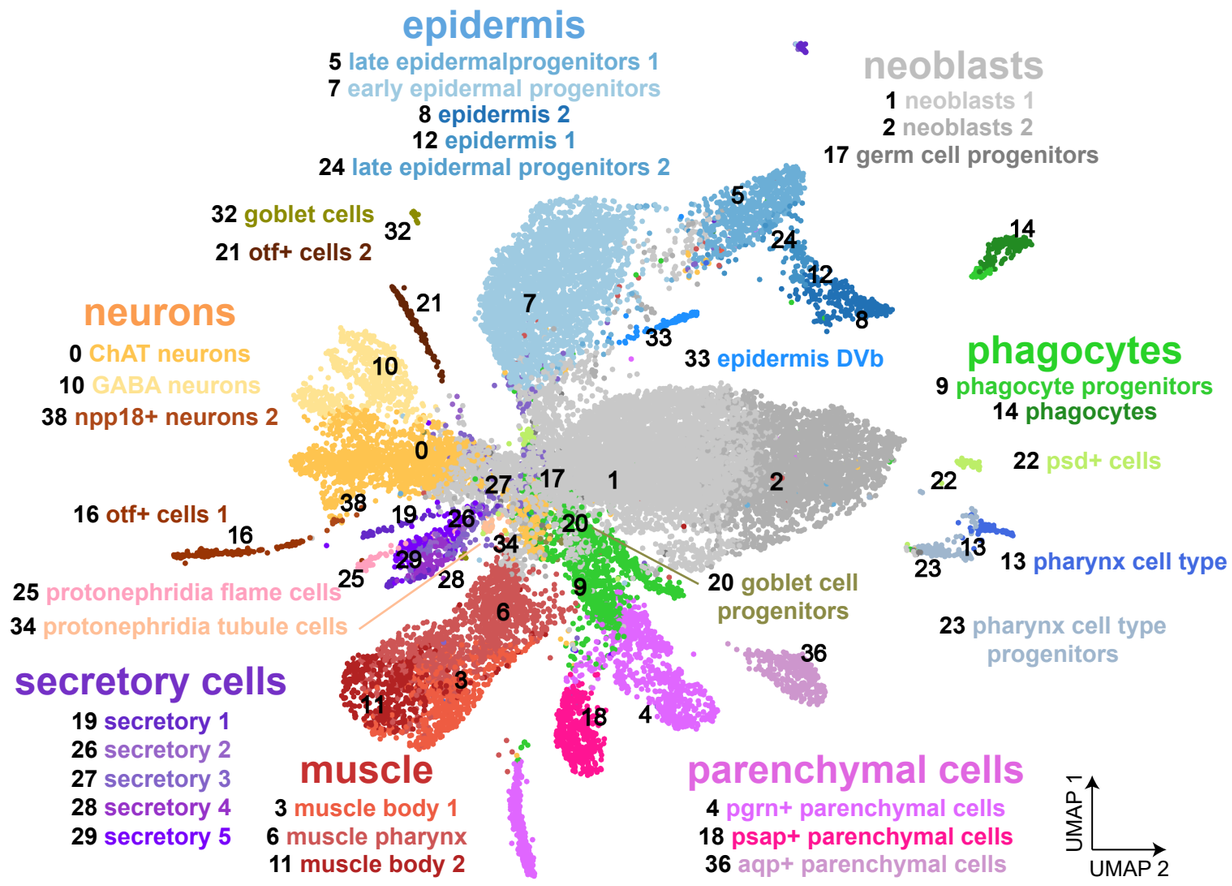

C

Trypsin-dissociated dataset (21,610 cells)
"Germ cell progenitors"
Labels transferred from this study

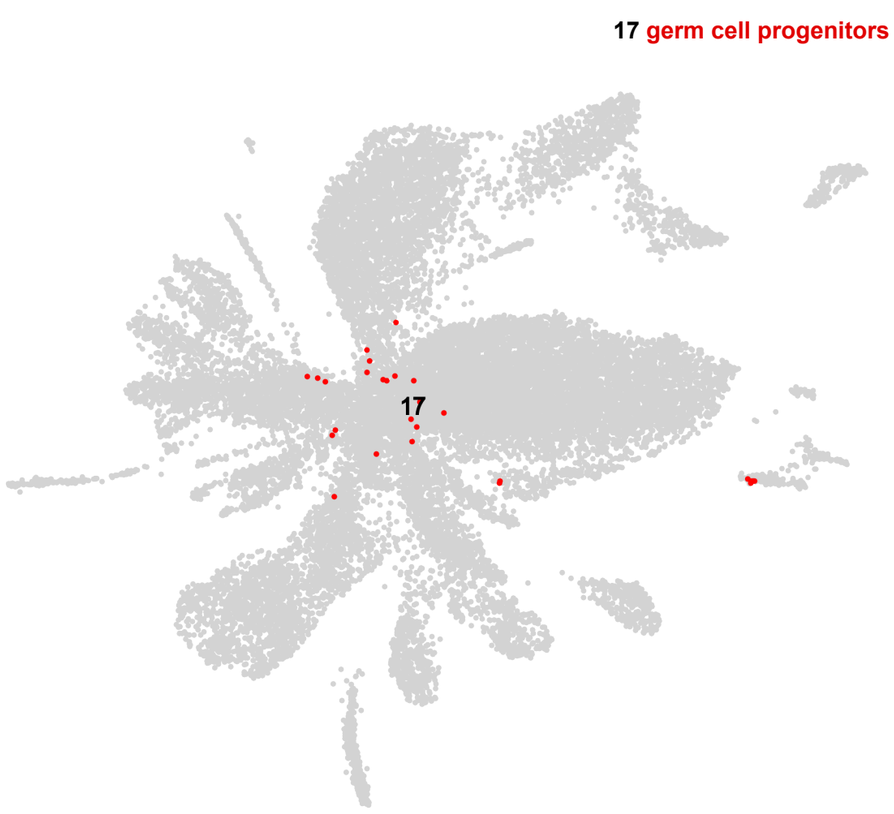

not transferred 15 neoblasts 3 30 serotonin neurons 31 npp-18+ neurons 1 35 secretory 6 37 cav-1+ neurons 39 eye-53 neurons 40 neoblast 4

D

***Smed-elF3c* (HM055595)**

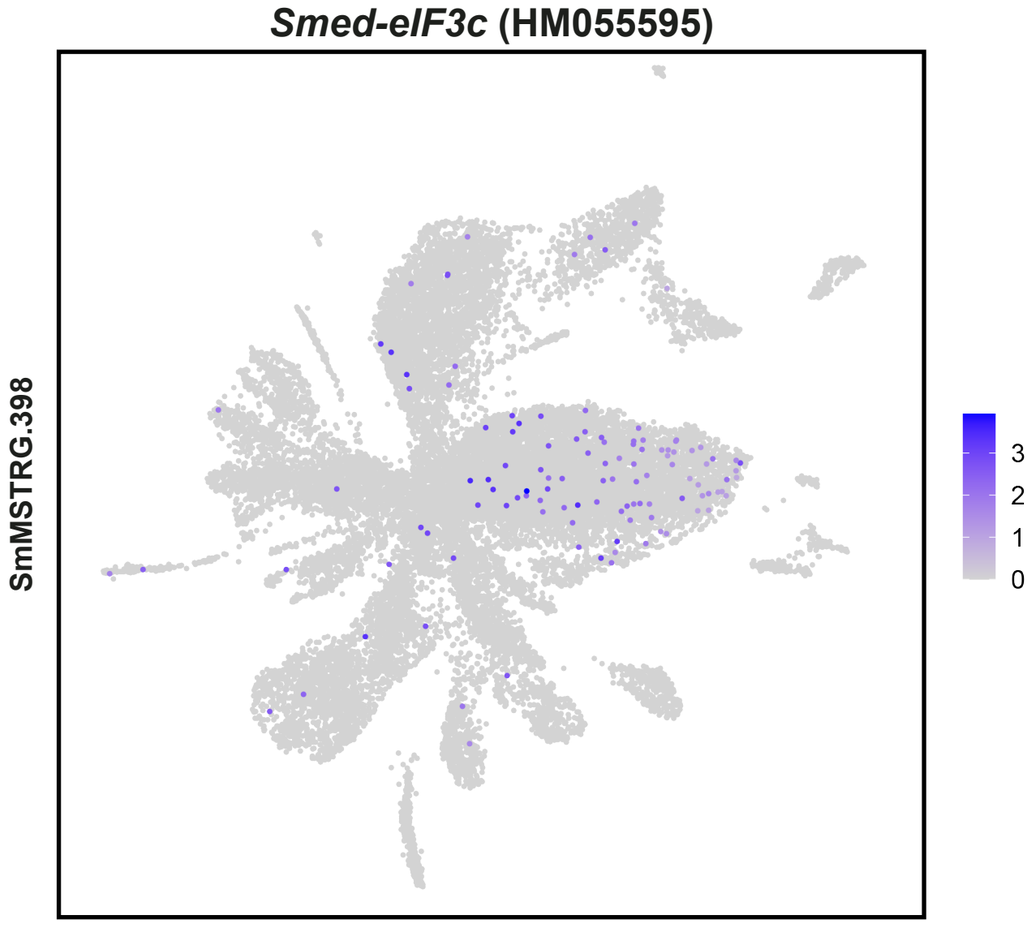

***Smed-nanos* (EF035555)**

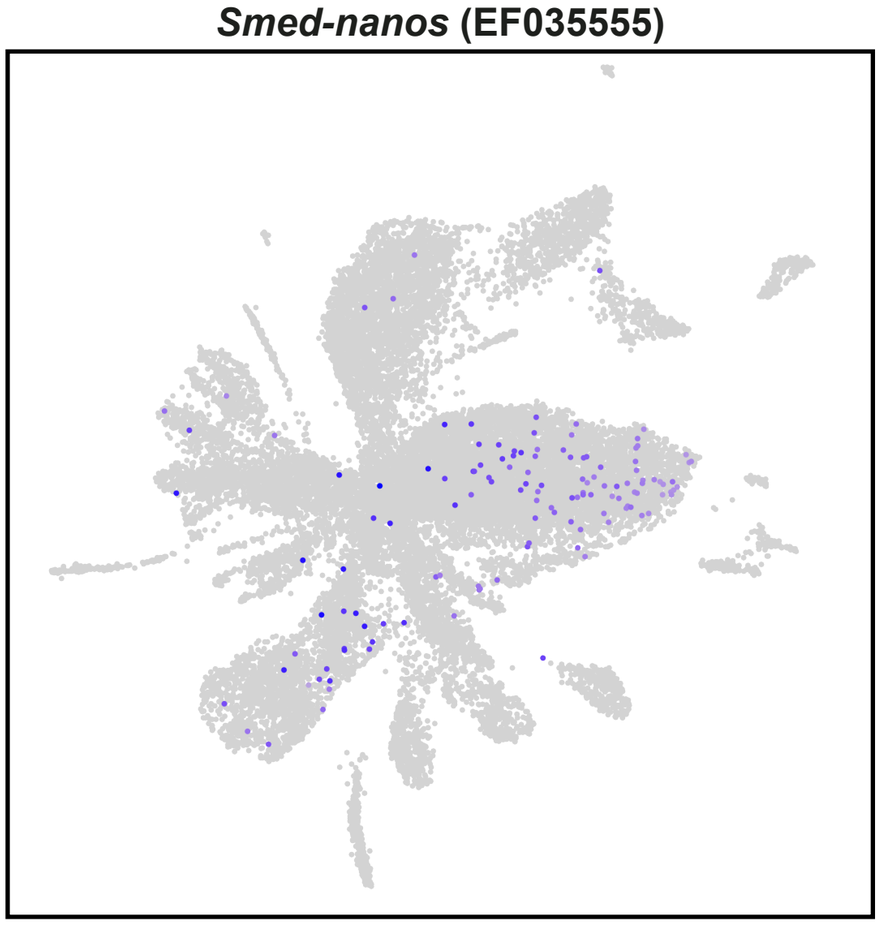

E Data Integration Labels transferred from Plass *et al*.